GEOSPHERE

GEOSPHERE; v. 11, no. 4

doi:10.1130/GES01153.1

17 figures; 4 supplemental files

CORRESPONDENCE: sekbennett@usgs.gov

CITATION: Bennett, S.E.K., Oskin, M.E., Dorsey, R.J., Iriondo, A., and Kunk, M.J., 2015, Stratigraphy and structural development of the southwest Isla Tiburón marine basin: Implications for latest Miocene tectonic opening and flooding of the northern Gulf of California: Geosphere, v. 11, no. 4, doi:10.1130/GES01153.1.

Received 19 November 2014
Revision received 15 April 2015
Accepted 2 June 2015

Stratigraphy and structural development of the southwest Isla Tiburón marine basin: Implications for latest Miocene tectonic opening and flooding of the northern Gulf of California

Scott E.K. Bennett[1,2*], Michael E. Oskin[1], Rebecca J. Dorsey[3], Alexander Iriondo[4,5], Michael J. Kunk[6]

[1]Department of Earth and Planetary Sciences, University of California–Davis, 2119 Earth and Physical Sciences, One Shields Avenue, Davis, California 95616, USA
[2]U.S. Geological Survey, Geologic Hazards Science Center, PO Box 25046, MS-966, Denver, Colorado 80225, USA
[3]Department of Geological Sciences, University of Oregon, 1272 University of Oregon, Eugene, Oregon 97403-1272, USA
[4]Centro de Geociencias, Universidad Nacional Autónoma de México, Campus Juriquilla, C.P. 76230 Juriquilla, Querétaro, México
[5]The University of Texas at Austin, Jackson School of Geosciences, 2305 Speedway, Stop C1160, Austin, Texas 78712, USA
[6]U.S. Geological Survey, 12201 Sunrise Valley Drive, MS-926A, Reston, Virginia 20192-0002, USA

ABSTRACT

Accurate information on the timing of earliest marine incursion into the Gulf of California (northwestern México) is critical for paleogeographic models and for understanding the spatial and temporal evolution of strain accommodation across the obliquely divergent Pacific–North America plate boundary. Marine strata exposed on southwest Isla Tiburón (SWIT) have been cited as evidence for a middle Miocene marine incursion into the Gulf of California at least 7 m.y. prior to plate boundary localization ca. 6 Ma. A middle Miocene interpretation for SWIT marine deposits has played a large role in subsequent interpretations of regional tectonics and rift evolution, the ages of marine basins containing similar fossil assemblages along ~1300 km of the plate boundary, and the timing of marine incursion into the Gulf of California. We report new detailed geologic mapping and geochronologic data from the SWIT basin, an elongate sedimentary basin associated with deformation along the dextral-oblique La Cruz fault. We integrate these results with previously published biostratigraphic and geochronologic data to bracket the age of marine deposits in the SWIT basin and show that they have a total maximum thickness of ~300 m. The 6.44 ± 0.05 Ma (Ar/Ar) tuff of Hast Pitzcal is an ash-flow tuff stratigraphically below the oldest marine strata, and the 6.01 ± 0.20 Ma (U/Pb) tuff of Oyster Amphitheater, also an ash-flow tuff, is interbedded with marine conglomerate near the base of the marine section. A dike-fed rhyodacite lava flow that caps all marine strata yields ages of 3.51 ± 0.05 Ma (Ar/Ar) and 4.13 ± 0.09 Ma (U/Pb) from the base of the flow, consistent with previously reported ages of 4.16 ± 1.81 Ma (K-Ar) from the flow top and (K-Ar) 3.7 ± 0.9 Ma from the feeder dike. Our new results confirm a latest Miocene to early Pliocene age for the SWIT marine basin, consistent with previously documented latest Miocene to early Pliocene (ca. 6.2–4.3 Ma) planktonic and benthic foraminifera from this section. Results from biostratigraphy and geochronology thus constrain earliest marine deposition on SWIT to ca. 6.2 ± 0.2 Ma, coincident with a regional-scale latest Miocene marine incursion into the northern proto–Gulf of California. This regional marine incursion flooded the northernmost, >500-km-long portion of the Gulf of California shear zone, a narrow belt of localized strike-slip faulting, clockwise block rotation, and subsiding pull-apart basins. Oblique Pacific–North America relative plate motion gradually localized in the >1000-km-long Gulf of California shear zone ca. 9–6 Ma, subsequently permitting the punctuated south to north flooding of the incipient Gulf of California seaway.

*Current address: U.S. Geological Survey, Department of Earth and Space Sciences, University of Washington, Box 351310, Seattle, Washington 98195, USA.

INTRODUCTION

Oblique rifting of the Baja California microplate away from mainland Mexico (North America plate) has created a system of ancient marine pull-apart basins, forming the early Gulf of California–Salton Trough topographic depression (Fig. 1A; Lonsdale, 1989). Fragments of the earliest marine basins, now exposed along the margins of the modern Gulf of California, beneath Colorado River sediments in the Salton Trough, and along the southern Colorado River corridor preserve an important record of the earliest marine conditions during localization of the plate boundary (Carreño, 1992; Martín-Barajas et al., 1997; McDougall et al., 1999; Holt et al., 2000; Oskin and Stock, 2003a; Miranda-Avilés et al., 2005; Dorsey et al., 2007, 2011; Miller and Lizarralde, 2013; McDougall and Miranda Martínez, 2014). Marine seismic reflection data have shown that marine basin formation and subsidence migrated westward as the northern Gulf of California opened (Aragón-Arreola and Martín-Barajas, 2007). Therefore, the earliest evidence of marine conditions may be preferentially preserved along the eastern (North America) rifted margin. Marine sedimentary and volcanic rocks on the southwestern corner of Isla Tiburón (Fig. 1B; Gastil and Krummenacher, 1977a, 1977b), in the southwest Isla Tiburón basin

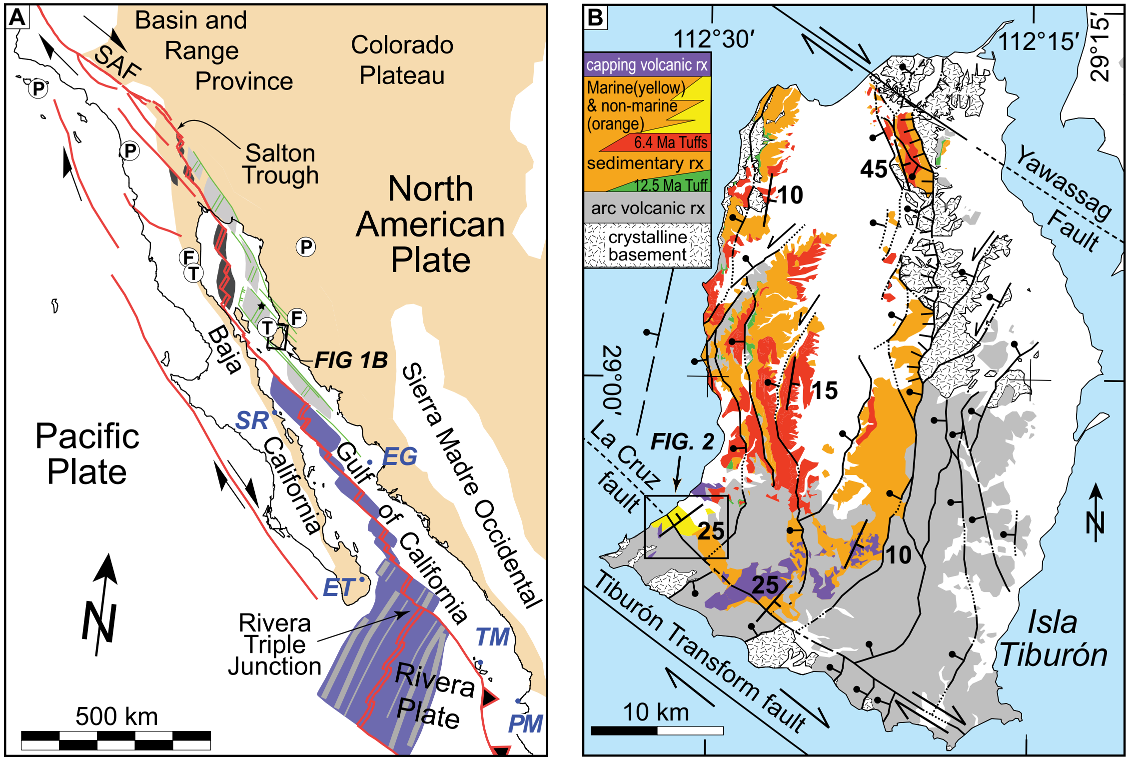

Figure 1. (A) Regional tectonic map of western North America showing the diffuse boundary between the Pacific–North American lithospheric plates (after Oskin and Stock, 2003b; Aragón-Arreola and Martín-Barajas, 2007; Fletcher et al., 2007). Active faults and spreading centers are red; inactive are green. Active pull-apart basins are dark gray; inactive are light gray. Pliocene–Quaternary hybrid oceanic crust and sediments are solid purple. Basaltic ocean crust is purple with gray normal polarity magnetic seafloor anomalies. SAF—San Andreas fault. Southern Gulf of California late Miocene marine rock localities: SR—Santa Rosalia; EG—East Guaymas Basin; ET—El Torote Ranch; TM—Tres Marías Islands; PM—Punta Mita. Cross-gulf tie points: P—Poway conglomerate (Abbott and Smith, 1989); F—fusulinid-rich clast conglomerate (Gastil et al., 1973); T—tuff sequence (Oskin et al., 2001; Oskin and Stock, 2003a). (B) Geologic map of Isla Tiburón; rx—rocks. (Geology was compiled from Gastil and Krummenacher, 1977a; Oskin, 2002; this study.)

(Oskin and Stock, 2003a), represent the only exposed Miocene marine record along the eastern margin of the northern Gulf of California. This southwest Isla Tiburón (SWIT) marine basin is located on North American continental crust and is a small subaerial exposure of the larger offshore upper Tiburón marine basin (Fig. 1). Examining the SWIT marine basin is critical for understanding the timing and tectonic controls of earliest marine conditions in the Gulf of California and for documenting rift architecture and oblique rifting processes that lead to recent rift localization. Globally, such subaerially exposed records of continental breakup are rare, commonly concealed by kilometers of water and sediment at mature rifted (passive) margins.

The role of the SWIT marine basin in understanding the evolution of the Gulf of California has been the subject of decades of study (Gastil and Krummenacher, 1977a, 1977b; Gastil et al., 1999; Oskin and Stock, 2003a), but the timing of initial marine conditions on SWIT remains controversial. A group of studies concluded that SWIT marine deposits are middle Miocene in age, bracketed between ca. 15 and 11 Ma volcanic units (Gastil and Krummenacher, 1977a, 1977b; Gastil et al., 1979, 1999; Smith et al., 1985; Smith, 1991). Gastil et al. (1999) documented an assemblage of marine microfossils from the SWIT marine deposits that are latest Miocene to Pliocene age (6.2–4.3 Ma), but did not integrate their biostratigraphic data into their middle Miocene interpretation for the SWIT marine basin. Oskin and Stock (2003a) suggested that a middle Miocene interpretation for SWIT marine deposits results from erroneous geochronologic (K-Ar) results and misinterpretation of crosscutting field relationships due to incomplete documentation of complex structural and stratigraphic relationships. Oskin and Stock (2003a) reinterpreted the timing of the SWIT marine basin to be late Miocene to Pliocene (6–4 Ma), consistent with the microfossil assemblage of Gastil et al. (1999). These conflicting interpretations for the age of the SWIT marine basin prevent a complete understanding of the geodynamic conditions of oblique rifting that led to marine incursion in the Gulf of California.

In this study we report the results of a multidisciplinary stratigraphic, structural, and geochronologic study of the SWIT marine basin. New constraints on timing and structural controls of basin formation, integrated with previously published results, yield a conclusive latest Miocene age (6.2 ± 0.2 Ma) for the earliest marine deposits on SWIT. This result is locally consistent with microfossil assemblages reported from the basin (Gastil et al., 1999) and regionally consistent with the well-documented record of a latest Miocene (ca. 6.3 Ma) marine incursion into the northern Gulf of California and Salton Trough (McDougall et al., 1999; Oskin and Stock, 2003a; Pacheco et al., 2006; Dorsey et al., 2007, 2011). Importantly, our results contradict previous interpretations for an older (pre–11 Ma), middle Miocene marine history in the northern Gulf of California. Instead, the data presented here support a latest Miocene age for marine incursion into the Gulf of California that was coincident in both time and space with strike-slip faulting and basin development along the Gulf of California shear zone in response to localization of transtensional strain across the Pacific–North America plate boundary.

PREVIOUS WORK AND CONTRADICTORY RESULTS

Well-documented exposures of marine strata record late Miocene south to north invasion of marine waters into the Gulf of California rift basin. At Punta Mita, Nayarit, along the southeastern margin of the Gulf of California (Fig. 1A), marine sedimentary rocks are interbedded with ca. 10 Ma basalt flows (Jensky, 1975; Gastil and Krummenacher, 1978). On the Tres Marías Islands (Carreño, 1985; McCloy et al., 1988) and at El Torote Ranch near the tip of Baja California (Molina-Cruz, 1994), marine conditions existed shortly prior to ca. 8–7 Ma, based on biostratigraphic age constraints. Farther north, ca. 7 Ma marine strata exposed near Santa Rosalia, Baja California Sur (Holt et al., 2000; Conly et al., 2005) are thought to be correlative to marine strata observed in geophysical lines in the eastern Guaymas Basin (Miller and Lizarralde, 2013). Earliest marine deposits exposed in Baja California Norte and southern California are distinctly younger than the central and southern Gulf of California, with biostratigraphic, isotopic, and paleomagnetic ages between 6.5 and 6 Ma (Boehm, 1984; Dean, 1996; McDougall et al., 1999; Escalona-Alcázar et al., 2001; Pacheco et al., 2006; Dorsey et al., 2007, 2011). In some localities, marine strata overlie middle Miocene volcanic rocks (e.g., Eberly and Stanley, 1978, as cited *in* McDougall, 2008; Delgado-Argote et al., 2000), providing only a maximum age for marine incursion. Elsewhere, broader timing constraints from microfossil assemblages are compatible with a latest Miocene marine incursion into the northern Gulf of California, Salton Trough, and lower Colorado River corridor region (e.g., McDougall and Miranda Martínez, 2014).

Evidence for earlier, middle Miocene (ca. 13–11 Ma) marine conditions in the central and northern Gulf of California also exists (e.g., Helenes and Carreño, 1999). Reworked microfossils reported from outcrop samples (McDougall et al., 1999; McDougall, 2008) and borehole cuttings (Helenes and Carreño, 1999; Helenes et al., 2009) provide indirect biostratigraphic evidence for middle Miocene marine deposits, presumably eroded from elsewhere in the Gulf of California or southern California region. Helenes et al. (2009) also reported in situ microfossils from borehole cuttings from the northern Gulf of California. Erosion of these strata could be the source of reworked fossils elsewhere.

Another unresolved issue is where to connect a middle Miocene seaway to the Pacific Ocean. Basal marine strata near the mouth of the Gulf of California are demonstrably younger, contradicting a southern seaway connection. This has led to the hypothesis of transpeninsular marine seaways across the central Baja California peninsula (e.g., Helenes and Carreño, 1999). Two such middle Miocene transpeninsular seaways are topographically plausible, assuming certain subsequent rift-flank uplift rates (Dolby et al., in press). However, these proposed seaways lack confirmation from geologic evidence, such as marine deposits preserved in candidate topographic passes.

The only isotopic age constraints for proposed middle Miocene marine deposits in the Gulf of California come from volcanic rocks that are interbedded with marine strata and overlie them on SWIT. Gastil and Krummenacher (1977b) reported an 11.2 ± 1.3 Ma (K-Ar) age for a subhorizontal rhyodacite lava flow that caps all marine deposits, interpreted as a minimum age constraint for the SWIT marine basin. Smith et al. (1985) later visited the island, and reported a 12.9 ± 0.4 Ma (K-Ar) age for a clast from a monolithologic andesitic breccia deposit interpreted to be interbedded with nearby exposures of marine conglomerate. This age corroborated Gastil and Krummenacher's (1977b) interpretation of a middle Miocene age for SWIT marine deposits. Neuhaus (1989) reported numerous K-Ar ages of ca. 21–15 Ma on arc-related volcanic rocks that underlie the SWIT marine deposits, and ages of ca. 6–4 Ma for tuffs and dikes interpreted to intrude and/or overlie the marine deposits. Gastil et al. (1999) summarized this earlier work and reported additional geochronologic and paleontological data for SWIT, including a late Miocene to Pliocene (6.2–4.3 Ma) assemblage of marine microfossils. Gastil et al. (1999) concluded that marine conditions were present in the SWIT basin as early as 13–12 Ma. The middle Miocene interpretation for SWIT marine deposits has played a prominent role in age interpretations of other basins throughout the Gulf of California region (e.g., Smith, 1991).

A middle Miocene interpretation for the SWIT basin and the concept of a middle Miocene Gulf seaway were challenged by Oskin and Stock (2003a), who suggested that this interpretation was based on incorrect dates and field interpretations. Neuhaus (1989) reported a 5.67 ± 0.17 Ma (K-Ar) age for a volcanic unit from SWIT and interpreted it to be a dike-fed rhyolite flow that postdates all marine strata. Geologic mapping (Oskin and Stock, 2003a) demonstrated that this volcanic unit is instead a pyroclastic flow deposit (tuff) interbedded at the base of the marine section. Oskin and Stock (2003a) suggested that the 11.2 ± 1.3 Ma age for the capping rhyolite lava flow was erroneous and that a 4.16 ± 1.81 Ma age (K-Ar) (Neuhaus, 1989) and a 3.7 ± 0.9 Ma age (K-Ar) (Gastil and Krummenacher, 1977b), both originally interpreted to have been collected from a set of younger, crosscutting dikes, are more likely representative ages for the capping rhyodacite lava flow and its feeder dike. Oskin and Stock (2003a) also proposed that the 12.9 ± 0.4 Ma andesitic breccia of Smith et al. (1985) is not interbedded with marine strata, and was unknowingly collected from underlying volcanic units exposed in an erosional window through the younger marine deposits, and concluded that the SWIT marine basin is late Miocene to Pliocene in age. However, in Oskin and Stock (2003a) no new age constraints were reported, and structural and stratigraphic relationships were not documented in sufficient detail to fully resolve the controversy over the age of the marine deposits in this area. Here we address these unresolved and controversial relationships from new structural, stratigraphic, and geochronologic results from the SWIT marine basin.

METHODS

Geologic, Structural, and Stratigraphic Mapping

We conducted 27 days of detailed geologic, structural, and stratigraphic mapping on SWIT during March 2009 and March–April 2011 (Figs. 2 and 3). Structural measurements include documentation of brittle fault orientations and kinematic indicators such as fault striae preserved on polished fault planes (Fig. 2). Mapping was conducted at a scale of 1:10000 on QuickBird satellite imagery with topographic contours derived from the 90 m Shuttle Radar Topography Mission digital elevation model (Farr et al., 2007). Three visible bands and one near-infrared band of QuickBird imagery were pan-sharpened to generate a 0.6-m-resolution false-color base map composed of near-infrared (760–900 nm), green (520–600 nm), and red (450–520 nm) spectral bands. Mapping at 1:5000 and 1:1000 scales was conducted in several portions of the study area that contain complex structural and stratigraphic relationships. Such high-resolution topography and satellite imagery were not available during all previous mapping efforts on SWIT. To assist with location descriptions, we refer to and number the seven modern-day streams (arroyos 0–6) that flow northwest through the study area into the Gulf of California, expanding upon the arroyo naming system of Gastil et al. (1999). Arroyo 0 is west of a prominent peak, Hast Pitzcal (Fig. 2), held up by the rhyodacite flow that caps the marine strata (a peak referred to as Cerro Starship in previous publications). Arroyos 1–6 are sequentially found east of Hast Pitzcal from southwest to northeast across the study area (Fig. 2).

Geochronology

To provide age constraints for marine deposits of the SWIT basin, we analyzed samples of volcanic units that underlie, are interbedded with, and overlie basin deposits. Samples typically consisted of 2–5 kg of fresh rock collected from representative, in-place outcrops. In the laboratory, samples were separated into their mineral constituents. Desired mineral phases for isotopic analysis were isolated via standard magnetic, density, and hand-picking mineral separation techniques. The U/Pb analysis of zircon crystals was conducted in the Laboratorio de Estudios Isotopicos, Centro de Geociencias, Universidad Nacional Autonoma de México (Querétaro), using an excimer laser coupled with a Thermo X-ii quadrupole inductively coupled plasma–mass spectrometer and following the analytical techniques reported by Solari et al. (2010). Zircon zoning was observed using cathodoluminescence imagery and crystal rims were targeted during multiple single-crystal analyses to avoid older inherited crystal cores. Typical sample spot beam locations varied between 23 and 32 μm in diameter. The Ar/Ar analysis of K-feldspar crystals and volcanic matrix was conducted in the U.S. Geological Survey Thermochronology Laboratory facility (Reston, Virginia). Multiple single-crystal analyses were conducted to allow detection of older inherited sanidine crystal populations. For all geochronologic results, we report ages with high precision (e.g., uncertainties of ≤3%).

GEOLOGY OF SWIT

The first geologic map and report of Isla Tiburón (Gastil and Krummenacher, 1977a, 1977b) documented the fundamental geologic relationships of the SWIT basin (Fig. 1), including Cretaceous crystalline basement nonconformably overlain by early to middle Miocene volcanic rocks, and the presence of dipping fossiliferous marine strata. Here we summarize the stratigraphy and geochronology of SWIT map units (Supplemental Table 1[1]) and the structures that deform these units.

Basement Rocks and Prerift Arc-Related Volcanic Rocks

Exposed basement rocks on SWIT consist entirely of Late Cretaceous (ca. 90–80 Ma) tonalite similar to outcrops on northeast Isla Tiburón (Gastil and Krummenacher, 1977a, 1977b; Schaaf et al., 1999; Niño-Estrada et al., 2014), southeast Isla Tiburón (Niño-Estrada et al., 2014), and along the adjacent Sonora coastline near Bahía de Kino (Gastil and Krummenacher, 1977a, 1977b; Ramos-Velázquez et al., 2008). In the SWIT study area, tonalite outcrops are observed only southwest of the La Cruz fault and are not exposed northeast of the fault (Figs. 2 and 3).

Thick deposits of prerift, early to middle Miocene arc-related volcanic rocks nonconformably overlie crystalline basement rocks on Isla Tiburón. Southwest of the La Cruz fault, the succession consists of red volcaniclastic sandstone, basalt flows and breccias, and lacustrine limestone. These are conformably overlain by additional basalt lava flows and breccias and volcaniclastic conglomerate. Previously reported ages range from ca. 23–15 Ma for these volcanic units (Fig. 2; Supplemental Table 1 [see footnote 1]; Gastil and Krummenacher, 1977b; Neuhaus, 1989; Gastil et al., 1999). Northeast of the La Cruz fault, the volcanic succession consists of interbedded dacite flows, dacite and andesite monolithologic breccias (Fig. 4A), and polylithologic andesitic breccias. Previously reported ages range from ca. 19–11 Ma for these volcanic units (Fig 2; Supplemental Table 1 [see footnote 1]; Gastil and Krummenacher, 1977b; Smith et al., 1985; Gastil et al., 1999).

An unconformity separates arc-related volcanic rocks from overlying synrift volcanic and sedimentary rocks (Fig. 3). The surface trace of this unconformity trends west-northwest–east-southeast across the study area (Fig. 2) and varies, as either a disconformity or angular unconformity. Given the

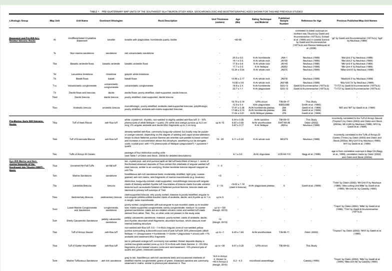

[1]Supplemental Table 1. Pre-Quaternary map units of the southwest Isla Tiburon study area. Geochronologic and biostratigraphic ages shown for this and previous studies. Please visit http://dx.doi.org/10.1130/GES01153.S1 or the full-text article on www.gsapubs.org to view Supplemental Table 1.

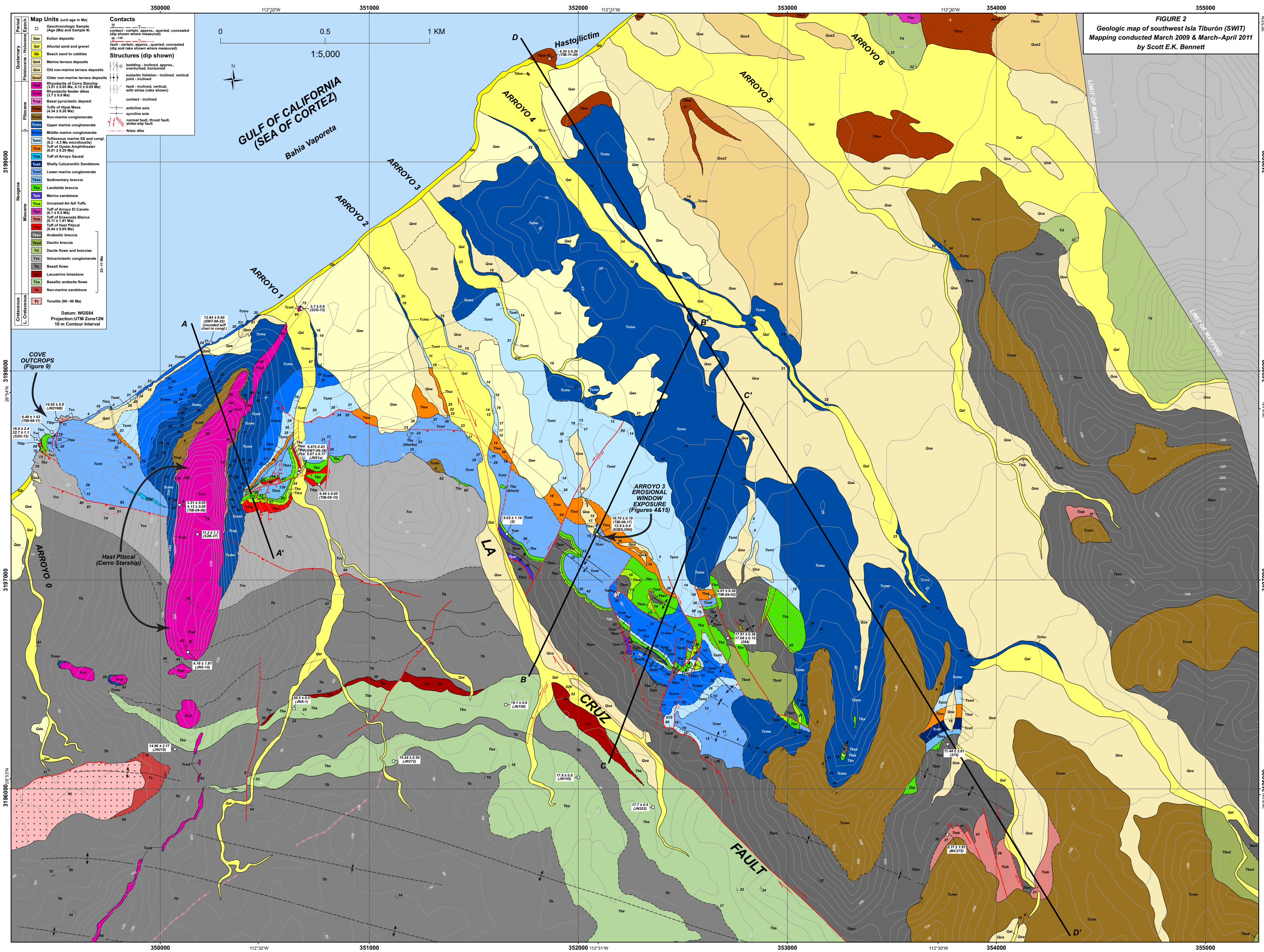

Figure 2. Geologic map of southwest Isla Tiburón (SWIT; scale 1:5,000; UTM—Universal Transverse Mercator, WGS84—World Geodetic System 1984). New and previously published geochronologic sample locations and isotopic ages shown. SS—sandstone; congl.—conglomerate; approx.—approximately; To download the large-format map plate, please visit http://dx.doi.org/10.1130/GES01153.S2 or the full-text article on www.gsapubs.org. Printed map sheet is 36″ tall, 48″ wide (~91 cm × 122 cm).

poor stratification within the arc-related volcanic rocks beneath this unconformity (e.g., Tvc, Tbxv), the degree of angularity is difficult to assess. Little to no weathering is observed in the units beneath this unconformity. In upper arroyo 3 we mapped an outcrop of andesitic breccia in an erosional window that exposes older, prerift volcanic rocks surrounded by unconformably overlying marine deposits (Fig. 2). Using a color copy of a field photo provided to us by J.T. Smith (2009, written commun.), and a field photo from Carreño and Smith (2007), we located the outcrop of andesitic breccia in this erosional window (Fig. 4B) and the very same breccia clast (Fig. 4C) for which Smith et al. (1985) reported a 12.9 ± 0.4 Ma (K-Ar) age. Zircons separated from our sample of this breccia clast yield a U/Pb age of 18.70 ± 0.19 Ma (Fig. 5A; Supplemental Table 2[2]), consistent with our mapping, which shows that this deposit belongs to middle Miocene, prerift, arc-related volcanic rocks that unconformably underlie the marine deposits.

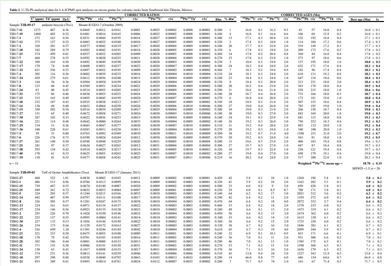

[2]Supplemental Table 2. U-Th-Pb analytical data for LA-ICPMS spot analyses on zircon grains for volcanic rocks from Southwest Isla Tiburón, México. Please visit http://dx.doi.org/10.1130/GES01153.S2 or the full-text article on www.gsapubs.org to view Supplemental Table 2.

Pre-Marine, Early Rift Volcanic Rocks

On SWIT, discontinuous outcrops of three distinct tuffs (Tthp, Tteb, Ttec) are mapped immediately above the unconformity that truncates middle Miocene arc-related volcanic rocks (Fig. 3). These tuffs differ in color, phenocryst assemblage and abundance, degree of welding, and number of cooling units (Supplemental Table 1 [see footnote 1]). The contact relationships of these tuffs with other units are incompletely known. The tuffs are not observed in contact with one another, and their geochronologic ages all overlap within uncertainty (Supplemental Table 1 [see footnote 1]).). Additionally, these tuffs are not in contact with marine deposits, and each is observed on only one side or the other of the La Cruz fault.

The tuff of Hast Pitzcal (Tthp) is a nonwelded to slightly welded ash-flow tuff observed discontinuously only southwest of the La Cruz fault, where it unconformably overlies arc-related volcanic rocks (Fig. 2) on both sides of arroyo 1 (Fig. 6) and just east of arroyo 0, in a small cove along the shoreline (Fig. 2). Sanidine crystals separated from a sample of Tthp yield an Ar/Ar age of 6.44 ± 0.05 Ma (Fig. 7A; Supplemental Table 3[3]). This age is consistent with an Ar/Ar age of 6.67 ± 0.83 Ma (Oskin, 2002) and similar to a K-Ar age of 5.67 ± 0.17 Ma (Neuhaus, 1989; Gastil et al., 1999) both from Tthp outcrops on the western side of arroyo 1 (Fig. 2; Supplemental Table 1 [see footnote 1]). The isotopic age, lithology, and phenocrysts of this tuff of Hast Pitzcal are strikingly similar to the Tmr3 cooling unit of the regionally extensive 6.4 Ma tuffs of Mesa Cuadrada (Oskin and Stock, 2003b). It is possible that the tuff of Hast Pitzcal may be a distal, nonwelded equivalent to this unit, which occurs as thick, densely welded tuff ~3 km northeast of arroyo 6 (Fig. 1B; Oskin 2002).

Table 3. $^{40}Ar/^{39}Ar$ laser total fusion data of single-crystal sanidine crystals from the Tuff of Hast Pitzcal, Southwest Isla Tiburón, México.

Hole number	$^{39}Ar_k$ (Moles)	Radiogenic Yield (%)	$^{40}Ar^*/^{39}Ar_k$	K/Ca	K/Cl	Age (Ma)	Error (Ma)
sample TIB-09-15	Tuff of Hast Pitzcal *(Ttha)*		***sanidine***	*J = 0.004411 ± 0.25%*		*#189KD53*	
15	6.27E-15	77.9	0.795	19.1	25000	6.32	± 0.05
23	4.22E-15	88.0	0.796	19.4	3125	6.32	± 0.07
16	5.96E-15	80.6	0.796	26.1	25000	6.33	± 0.04
1	8.74E-15	95.9	0.797	17.3	8333	6.33	± 0.04
21	6.08E-15	92.5	0.798	19.8	14286	6.34	± 0.03
12	4.11E-15	95.5	0.803	22.6	4545	6.38	± 0.09
5	4.56E-15	93.2	0.804	21.5	9091	6.39	± 0.08
8	5.59E-15	84.5	0.804	21.4	5882	6.39	± 0.07
13	6.19E-15	95.8	0.805	14.1	14286	6.39	± 0.03
17	5.26E-15	96.1	0.807	13.3	6667	6.41	± 0.04
7	5.90E-15	61.3	0.807	15.0	9091	6.41	± 0.08
22	8.93E-15	90.3	0.808	20.7	6667	6.41	± 0.03
2	6.70E-15	89.3	0.808	23.6	4545	6.42	± 0.05
10	4.85E-15	92.6	0.811	23.9	7692	6.44	± 0.08
30	5.11E-15	96.1	0.811	17.9	3448	6.44	± 0.04
32	4.85E-15	97.1	0.811	15.7	4348	6.45	± 0.04
4	8.16E-15	86.1	0.812	14.8	5556	6.45	± 0.05
28	4.88E-15	89.8	0.813	17.0	2381	6.46	± 0.04
11	5.67E-15	76.2	0.813	17.7	4545	6.46	± 0.07
14	5.00E-15	92.4	0.813	17.1	20000	6.46	± 0.04
9	3.59E-15	99.4	0.814	22.3	***	6.46	± 0.10
26	3.77E-15	88.0	0.814	16.6	11111	6.46	± 0.05
29	6.24E-15	98.7	0.814	14.2	8333	6.47	± 0.03
33	2.77E-15	95.2	0.815	15.7	7692	6.47	± 0.06
36	3.17E-15	66.5	0.816	18.2	10000	6.48	± 0.08
35	5.96E-15	92.3	0.817	16.5	2128	6.49	± 0.04
31	3.76E-15	97.3	0.818	19.2	3448	6.50	± 0.05
37	2.07E-15	99.5	0.821	21.5	5882	6.52	± 0.09
19	5.55E-15	93.9	0.822	24.6	3571	6.53	± 0.05
34	3.80E-15	96.0	0.822	17.1	9091	6.53	± 0.05
25	5.13E-15	96.6	0.824	17.4	3333	6.55	± 0.04
20	3.73E-15	43.0	0.825	20.2	4348	6.55	± 0.10
27	1.99E-15	94.2	0.828	16.4	2778	6.58	± 0.09
24	2.57E-15	97.3	0.839	16.9	2222	6.67	± 0.08
		MSWD = 1.47		**Weighted Mean Age =**		**6.44**	**± 0.05**

[3]Supplemental Table 3. $^{40}Ar/^{39}Ar$ laser total fusion data of single-crystal sanidine crystals from the Tuff of Hast Pitzcal, Southwest Isla Tiburón, México. Please visit http://dx.doi.org/10.1130/GES01153.S3 or the full-text article on www.gsapubs.org to view Supplemental Table 3.

The tuff of Ensenada Blanca (Tteb) is a densely welded ash-flow tuff that unconformably overlies arc-related volcanic rocks and is observed only northeast of the La Cruz fault in the upper reaches of arroyos 4 and 5 (Fig. 2). Neuhaus (1989) reported a 6.11 ± 1.81 Ma (K-Ar) whole-rock age from Tteb outcrops in arroyo 4. Tteb exposures are overlain in angular unconformable contact by nonmarine conglomerate deposits that we interpret to be coeval with the youngest marine deposits.

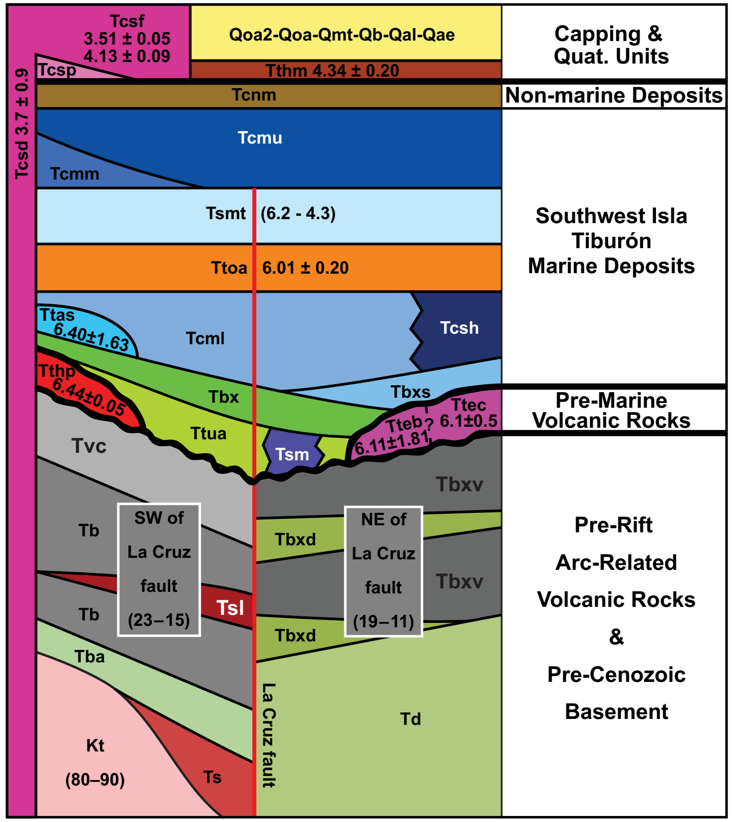

Figure 3. Schematic stratigraphic column of geologic map units on southwest Isla Tiburón, as mapped in Figure 2 (abbreviation as in Fig. 2 legend). Geochronologic and biostratigraphic ages are in Ma. See text for descriptions and isotopic ages of units. Quat.—Quaternary.

The tuffs of Arroyo El Canelo (Ttec), a package of four to six distinctive cooling units (Oskin and Stock, 2003b), locally overlie arc-related volcanic rocks northeast of the La Cruz fault and northeast of arroyo 6 (Fig. 2). This unit also overlies the 6.4 Ma tuffs of Mesa Cuadrada north of the study area (Oskin and Stock, 2003b). Nagy et al. (1999) reported a 6.1 ± 0.5 Ma (Ar/Ar) age for correlative Ttec outcrops in the Puertecitos volcanic province of northeastern Baja California. The outcrops mapped northeast of arroyo 6 are the southernmost distal exposures of the tuffs of Arroyo El Canelo documented on the eastern side of the Gulf of California.

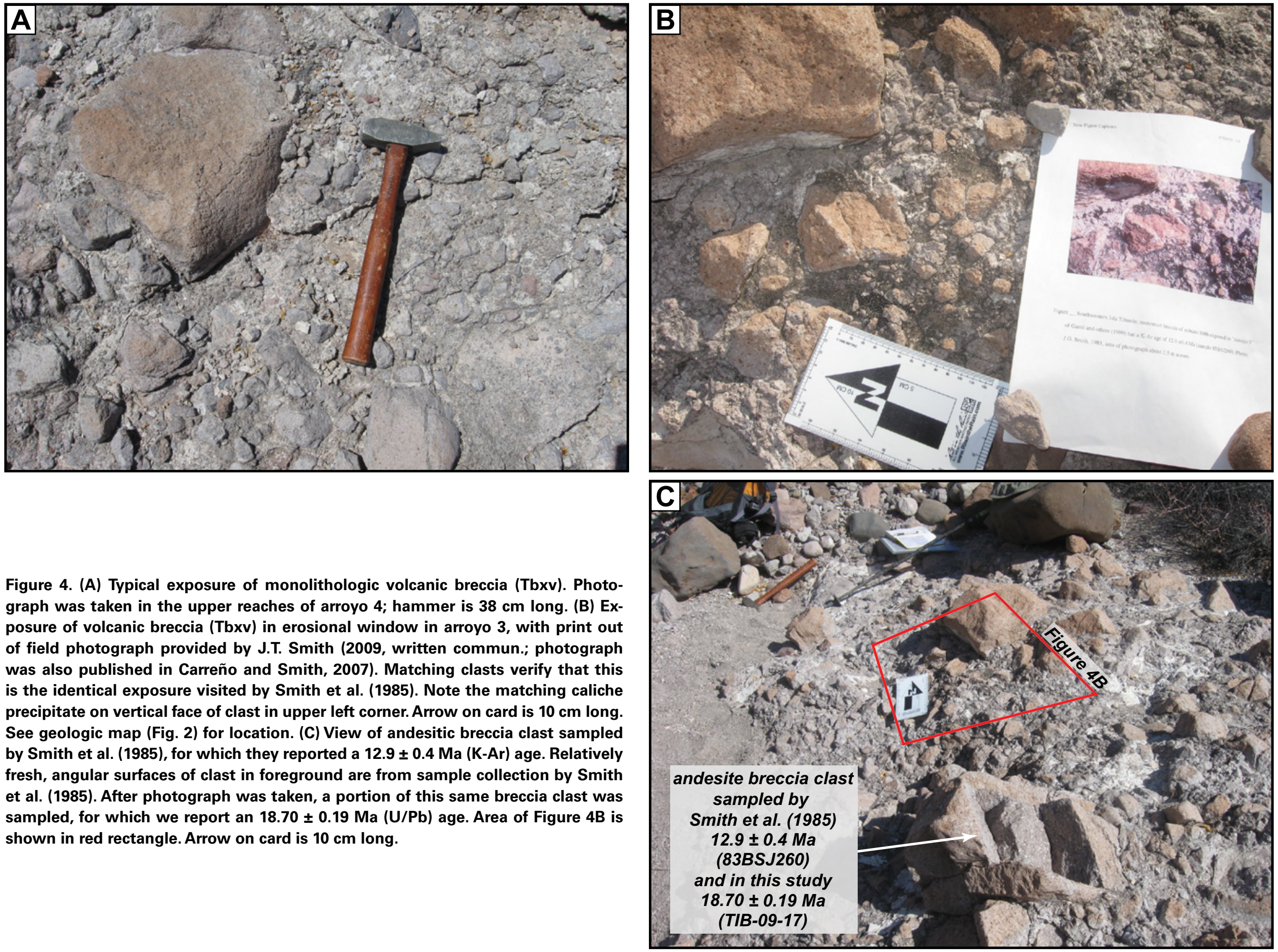

Figure 4. (A) Typical exposure of monolithologic volcanic breccia (Tbxv). Photograph was taken in the upper reaches of arroyo 4; hammer is 38 cm long. (B) Exposure of volcanic breccia (Tbxv) in erosional window in arroyo 3, with print out of field photograph provided by J.T. Smith (2009, written commun.; photograph was also published in Carreño and Smith, 2007). Matching clasts verify that this is the identical exposure visited by Smith et al. (1985). Note the matching caliche precipitate on vertical face of clast in upper left corner. Arrow on card is 10 cm long. See geologic map (Fig. 2) for location. (C) View of andesitic breccia clast sampled by Smith et al. (1985), for which they reported a 12.9 ± 0.4 Ma (K-Ar) age. Relatively fresh, angular surfaces of clast in foreground are from sample collection by Smith et al. (1985). After photograph was taken, a portion of this same breccia clast was sampled, for which we report an 18.70 ± 0.19 Ma (U/Pb) age. Area of Figure 4B is shown in red rectangle. Arrow on card is 10 cm long.

Synrift Marine and Nonmarine Deposits (SWIT Basin)

Marine sedimentary and volcanic rocks in the SWIT basin record earliest marine conditions on Isla Tiburón. Unlike the pre-marine synrift volcanic rocks, the majority of SWIT marine units are observed on both sides of the La Cruz fault.

A sequence of unnamed airfall tuff beds (Ttua; Fig. 8A) is discontinuously preserved at the base of the SWIT basin and is the oldest map unit mapped on both sides of the La Cruz fault (Figs. 2 and 3). No published radiometric age exists for Ttua; however, it conformably overlies the 6.44 ± 0.05 Ma tuff of Hast Pitzcal in outcrops adjacent to arroyo 1 (Fig. 2).

The oldest known marine deposits in the SWIT basin are laterally discontinuous, fossiliferous, ash-rich sandstone beds (Tsm) that unconformably overlie arc-related volcanic rocks. These strata are observed only northeast of the La Cruz fault, on the northeast side of arroyo 2 (Fig. 2). Deposits of Tsm are observed at the same stratigraphic level as Ttua, both overlain by a distinctive landslide breccia deposit (e.g., east side of arroyo 2), although Tsm and Ttua are nowhere observed in contact. The ash-rich matrix in Tsm could be sourced from the underlying Tthp and/or laterally equivalent airfall tuffs (Ttua).

A landslide breccia (Tbx) overlies arc-related volcanic rocks, the tuff of Hast Pitzcal (Tthp), marine sandstone (Tsm), and unnamed airfall tuffs (Ttua) (Figs.

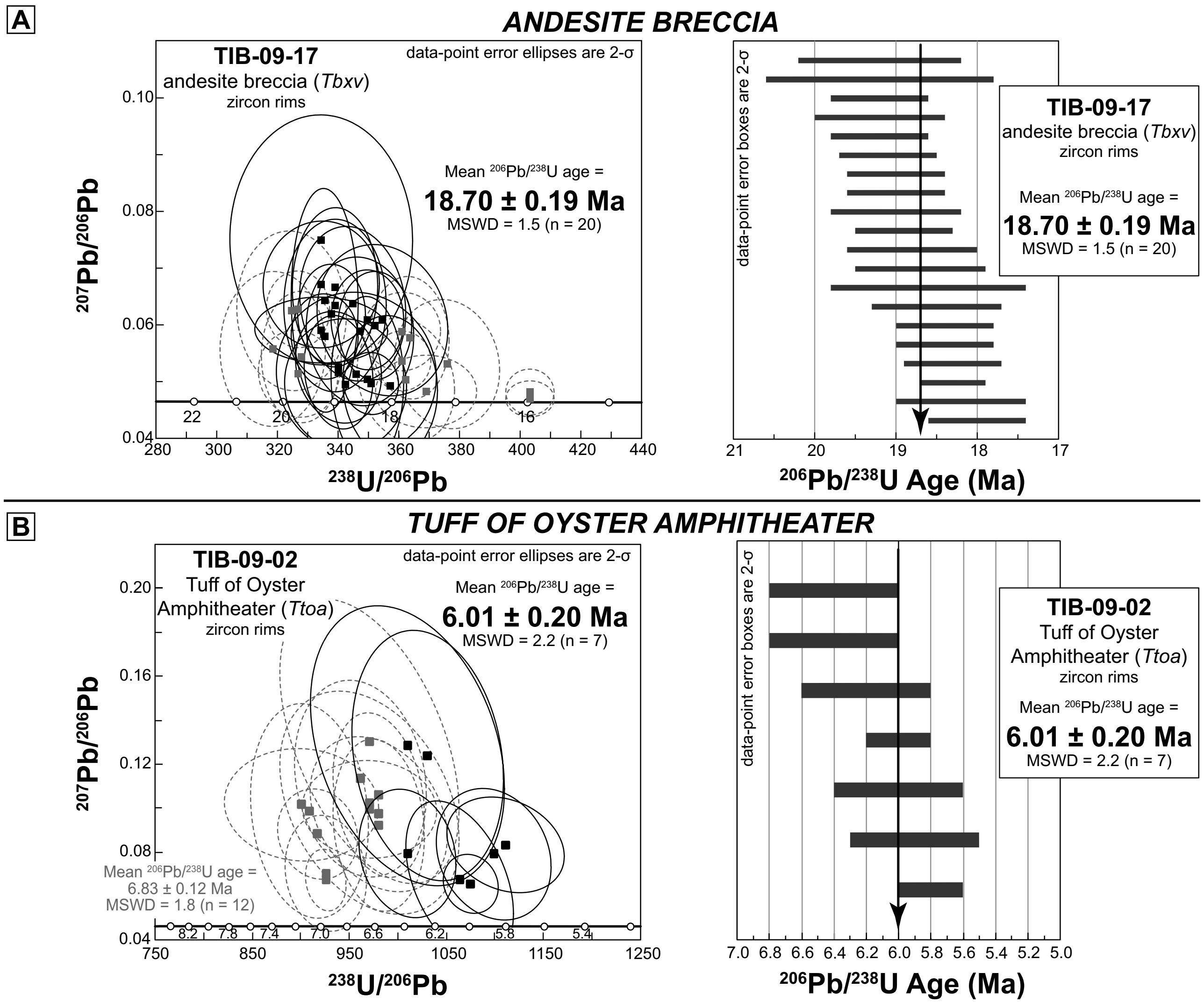

Figure 5 (*on this and following page*). $^{206}Pb/^{238}U$ zircon geochronologic ages calculated for volcanic rocks on southwestern Isla Tiburón (SWIT). Tera-Wasserburg concordia diagrams are on left and age spectrum diagrams are on right. MSWD—mean square of weighted deviates. (A) Andesite breccia (Tbxv) in arroyo 3 erosional window that underlies the SWIT marine basin. (B) Tuff of Oyster Amphitheater (Ttoa) interbedded within the marine basin.

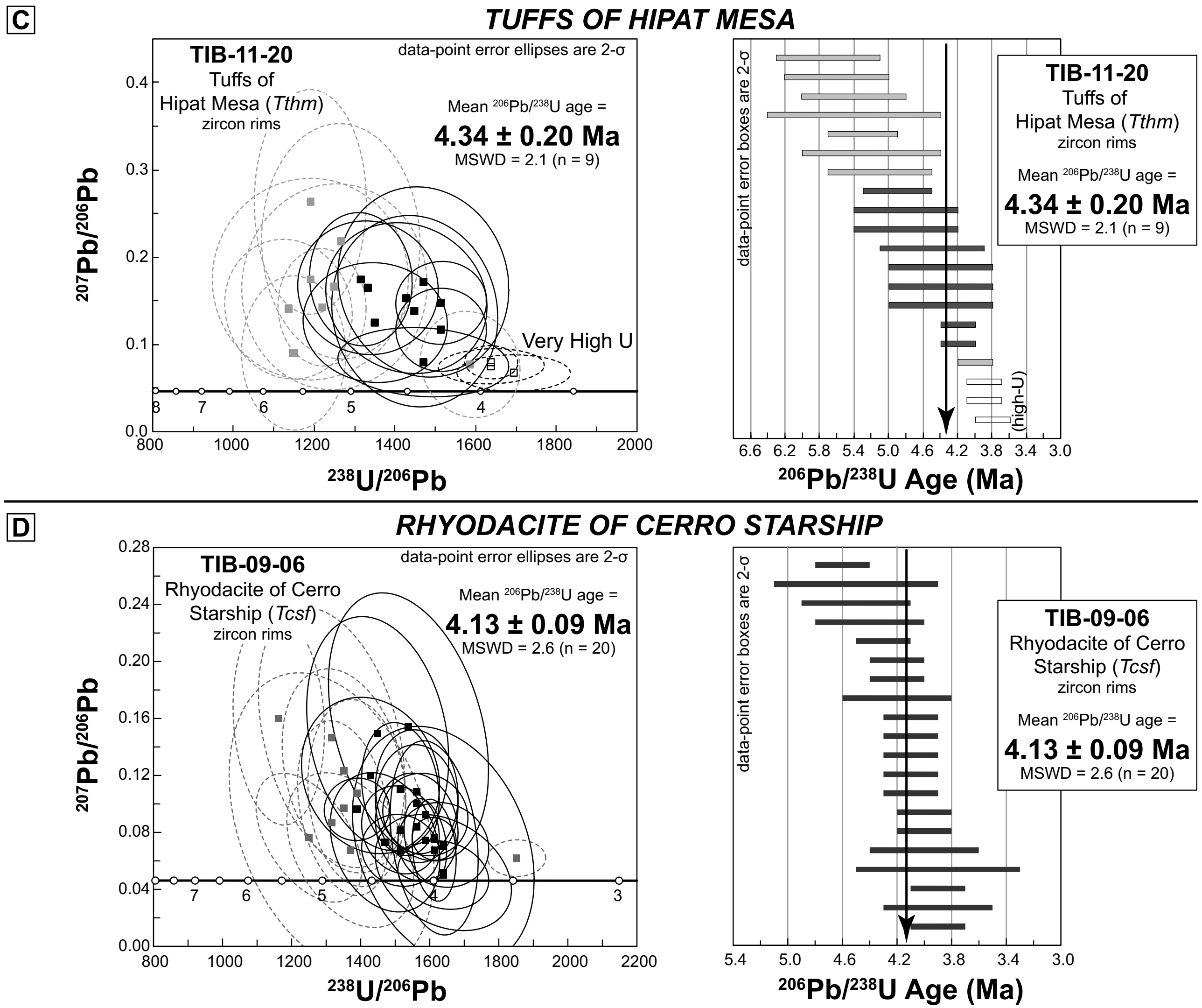

Figure 5 (*continued*). (C) Tuffs of Hipat Mesa (Tthm) that cap the marine basin. (D) Rhyodacite of Cerro Starship (Tcsf) that caps the marine basin. Zircon crystals omitted from mean age calculation are gray squares with gray, dashed error ellipses. Relatively younger zircons have high uranium concentrations (Supplemental Table 2 [see footnote 2]) and are omitted from mean age due to possible lead loss. Relatively older zircons are omitted due to potential inheritance. See Supplemental Table 2 (see footnote 2) for analysis data.

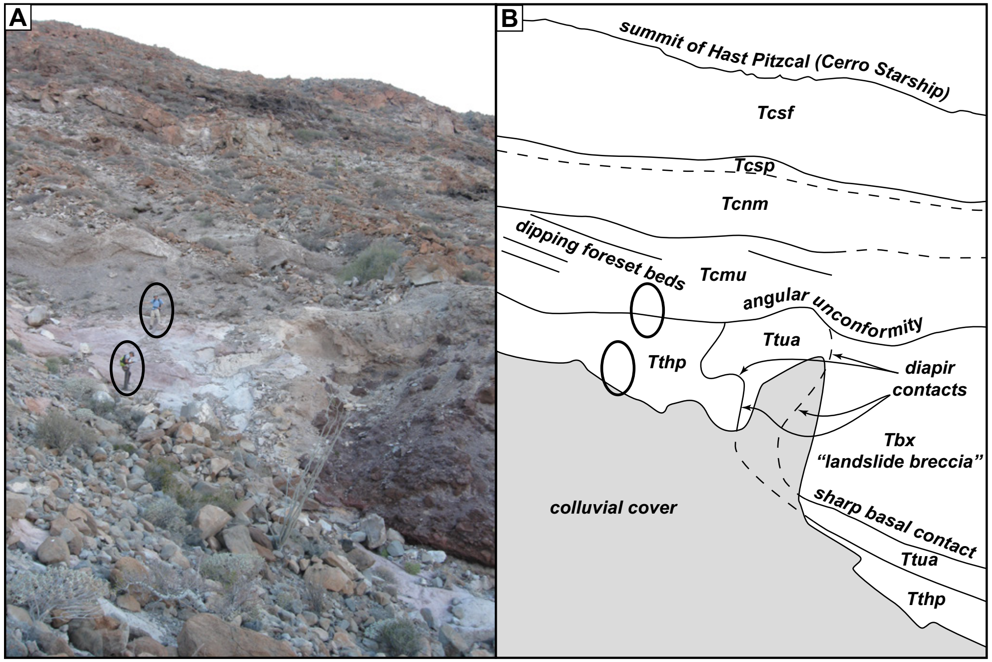

Figure 6. View of angular unconformity between pre-basin volcanic units (Tthp, Ttua, Tbx) and overlying marine deposits (Tcmu), nonmarine sediments (Tcnm), and volcanic units (Tcsp, Tcsf) (see text). Photograph taken looking northwest along eastern flank of Hast Pitzcal, west of arroyo 1. Circled geologists for scale.

2 and 3). Tbx forms a distinctive marker at or ~5 m stratigraphically above the base of the marine deposits and is laterally continuous across the study area except where locally absent at paleotopographic highs between arroyos 1 and 2 and in arroyo 4. Deposits of Tbx consist of distinctive, burgundy colored, clast-supported, monolithologic breccia with angular clasts of densely welded rhyolite tuff (Figs. 6, 8A, and 8B). The boundaries of breccia clasts truncate volcanic textures such as eutaxitic foliation of flattened pumice fiamme, indicating that this unit is sourced from an older ash-flow tuff that was fragmented after cooling and welding of the original deposit, and subsequently mobilized and emplaced as a breccia deposit (Oskin and Stock, 2003a). Clasts in Tbx are identical to primary tuff outcrops of Tteb in arroyo 4, suggesting that Tteb was the source of the landslide breccia (Tbx) and possibly also the source of similar, but thinner breccia units interstratified with the unnamed airfall tuffs (Ttua). Gastil et al. (1999) reported a 9.02 ± 1.18 Ma (Ar/Ar) plateau age on plagioclase crystals separated from a Tbx sample collected on the northeast side of arroyo 2. Although the error bounds for the reported ages for Tteb (6.11 ± 1.81 Ma) and Tbx barely overlap at ca. 7.9 Ma, they generally disagree. The spectra for the 9.02 ± 1.18 Ma (Ar/Ar) plateau age on Tbx were not published by Gastil et al. (1999), making it difficult to assess its reliability.

Sedimentary breccia deposits (Tbxs) discontinuously overlie the landslide breccia (Tbx) and older arc-related volcanic rocks in arroyos 1 and 4 (Fig. 2). Deposits of Tbxs (Fig. 8C) are interpreted to be the result of a debris flow or rock avalanche deposited in either a nonmarine or marginal-marine setting (Keogh, 2010).

Lower marine conglomerate and sandstone (Tcml) conformably overlie older units (e.g., Tbx and arc-related volcanic rocks; Fig. 9) at or near the base of the SWIT marine section (Figs. 2 and 3). Tcml deposits (Figs. 10A–10D) contain rare to common marine macrofossils, including the remnants of barnacle bases on clasts (Fig. 10E) and rare large oysters (Fig. 10F).

Shelly calcarenitic sandstone (Tcsh) locally overlies sedimentary breccia (Tbxs) and is observed only in the upper reaches of arroyo 4 (Fig. 2). Tcsh in arroyo 4 is likely laterally equivalent to lower conglomerate (Tcml), which is mapped at the same stratigraphic level along strike to the west-northwest (Figs. 2 and 3).

The tuff of Arroyo Sauzal (Ttas) overlies Tbx and forms discontinuous outcrops of nonwelded ash-flow tuff just east of arroyo 0, in a small cove at the shoreline where an Ar/Ar age of 6.40 ± 1.63 Ma (Oskin, 2002) was reported (Fig. 9), and higher up on the western flank of Hast Pitzcal (Fig. 2). Oskin and Stock (2003a) interpreted that *Ttas* was emplaced over an irregular paleotopographic surface formed by the underlying landslide breccia (Tbx) in a shoreline setting amongst Tcml deposits. Oskin and Stock (2003a) also correlated the tuff of Arroyo Sauzal outcrops in this coastal cove to outcrops of the tuff of Hast

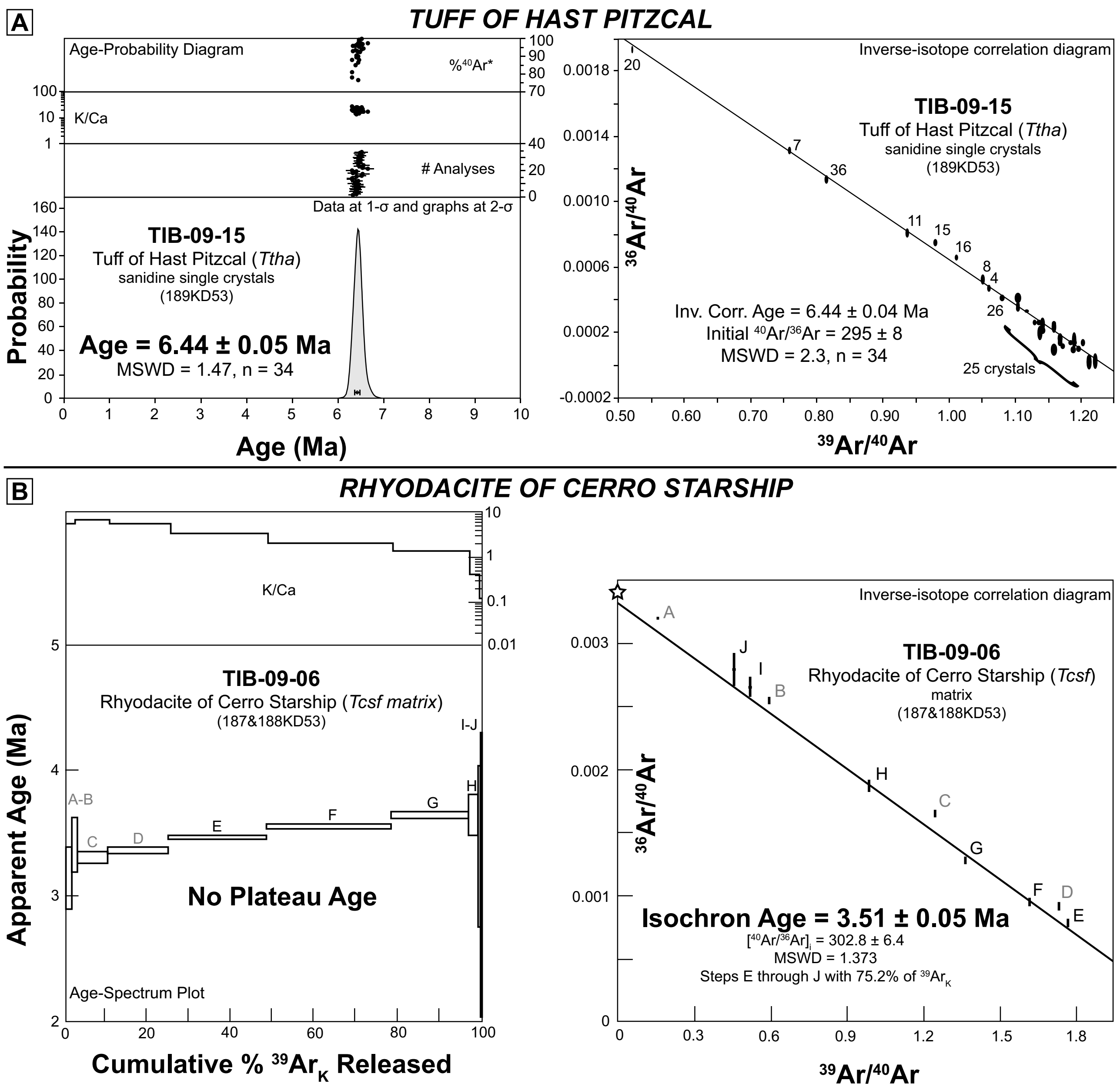

Figure 7. $^{40}Ar/^{39}Ar$ geochronologic ages calculated for volcanic rocks on southwestern Isla Tiburón (SWIT). (A) Percent $^{40}Ar^*$, K/Ca ratios, and age probability diagram of multiple single-grain total fusion ages on potassium-feldspar crystals (left) and inverse-isotope correlation diagram (right) for the tuff of Hast Pitzcal (Tthp) that immediately underlies the SWIT marine basin. See Supplemental Table 3 (see footnote 3) for analysis data. MSWD—mean square of weighted deviates. (B) K/Ca ratios and age spectrum plot (left) and inverse-isotope correlation diagram (right) for volcanic matrix of the Rhyodacite of Cerro Starship (Tcsf) that overlies the SWIT marine basin. Gray shaded letters indicate steps excluded from the isochron age determination. See Supplemental Table 4 (see footnote 4) for analysis data.

Pitzcal in arroyo 1, which were dated as 5.67 ± 0.17 Ma by Gastil et al. (1999) and redated in this study as 6.44 ± 0.05 Ma (Fig. 7A; Supplemental Table 3 [see footnote 3]). Our detailed mapping shows this correlation to be incorrect; the landslide breccia actually overlies the tuff of Hast Pitzcal in arroyo 1.

The tuff of Oyster Amphitheater (Ttoa) is an ash-flow tuff that conformably overlies marine conglomerate (Tcml) and laterally equivalent shelly calcarenitic sandstone (Tcsh). In most localities the tuff is nonwelded. We collected a sample of Ttoa from outcrops on the ridge between arroyo 3 and arroyo 4, adjacent to a topographic bowl that contains marine conglomerate with abundant oyster shell fossils. At this ridgeline, an ~20–30-m-thick interval of Ttoa exhibits a 5–10-m-thick core of slightly welded tuff. Ttoa is observed stratigraphically between marine sedimentary units, thus it is possible that it was emplaced in shallow marine water. Zircons separated from a sample from this welded zone yielded a U/Pb age of 6.01 ± 0.20 Ma (Fig. 5B; Supplemental Table 2 [see footnote 2]).

Marine tuffaceous sandstone (Tsmt) conformably overlies the tuff of Oyster Amphitheater (Ttoa). Ash-rich tuffaceous sandstone (Fig. 10G) likely represents the reworked portions of the underlying Ttoa. Unique grains of green, iridescent sanidine are commonly observed in Tsmt matrix, similar to phenocrysts observed in Ttoa. Previous reports of microfossil assemblages from Tsmt (unit Mss-Unit 4a of Cassidy, 1990; unit M8c of Gastil et al., 1999) included benthic and planktonic foraminifers, calcareous nannoplankton, and ostracodes that together restrict the age of Tsmt to 6.2–4.3 Ma (Gastil et al., 1999). Several (n = 17) species of benthic and planktonic foraminifers from Tsmt match species documented in the Whitewater, Cabazon, and Fish Creek–Vallecito marine deposits in the Salton Trough (McDougall et al., 1999; Dorsey et al., 2007; McDougall, 2008; K. McDougall, 2015, written commun.), where earliest marine deposition occurred ca. 6.3 ± 0.2 Ma. Only genus-level matches can be made with foraminifers from 8.1–5.3 Ma marine deposits in the lower Bouse Formation of the Blythe basin (McDougall and Miranda Martínez, 2014). Scattered macrofossils are also observed in Tsmt, including fragments of oysters, pectens, barnacles, gastropods, and echinoid spines and fragments (Figs. 10C, 10E, 10F, 10H; Cassidy, 1990; Gastil et al., 1999; this study). We observe abundant disarticulated specimens and fragments of the oyster *Pycnodonte heermanni* in Tsmt (identified by J. Smith, 2013, written commun.), which has a type locality near the Coyote Mountains of southern California, where marine deposits are demonstrably late Miocene (Dorsey et al., 2011). Stump (1979) also assigned a late Miocene age to this macrofossil assemblage from SWIT. Trace fossils in Tsmt in the form of subvertical burrows are rare (Fig. 10I).

Middle marine conglomerate and sandstone (Tcmm) conformably overlie tuffaceous marine sandstone (Tsmt), or, less commonly, older units where Tsmt is absent. Tcmm is similar to conglomeratic facies of Tsmt, but contains >50% conglomerate beds. Oskin (2002) reported an Ar/Ar age of 12.84 ± 0.40 Ma on a rounded clast of welded rhyolite tuff collected from Tcmm west of the mouth of arroyo 1 (Fig. 2). This clast was likely sourced from outcrops of the tuff of San Felipe, a ca. 12.5 Ma regional ash-flow tuff (Oskin and Stock, 2003b) exposed on Cerro Colorado, just southeast of the SWIT marine basin (Bennett, 2013).

Figure 8. Breccia units observed at base of southwestern Isla Tiburón (SWIT) marine basin. (A) Distinctive landslide breccia (Tbx) in sharp contact above unnamed air-fall tuffs (Ttua) (see text). Hammer for scale. Photograph from Neuhaus (1989). (B) Typical outcrop texture of distinctive landslide breccia deposit (Tbx). Eutaxitic foliation of flattened pumice fiamme is visible in large breccia clasts, similar to intact source outcrops of the tuff of Ensenada Blanca (Tteb). Hammer handle width is ~3.5 cm. (C) Typical outcrop of polylithologic sedimentary breccia (Tbxs) that discontinuously underlies marine deposits in arroyos 1 and 4. Photograph taken in the upper reaches of arroyo 4. Hammer is 38 cm long. Photograph is from Keogh (2010).

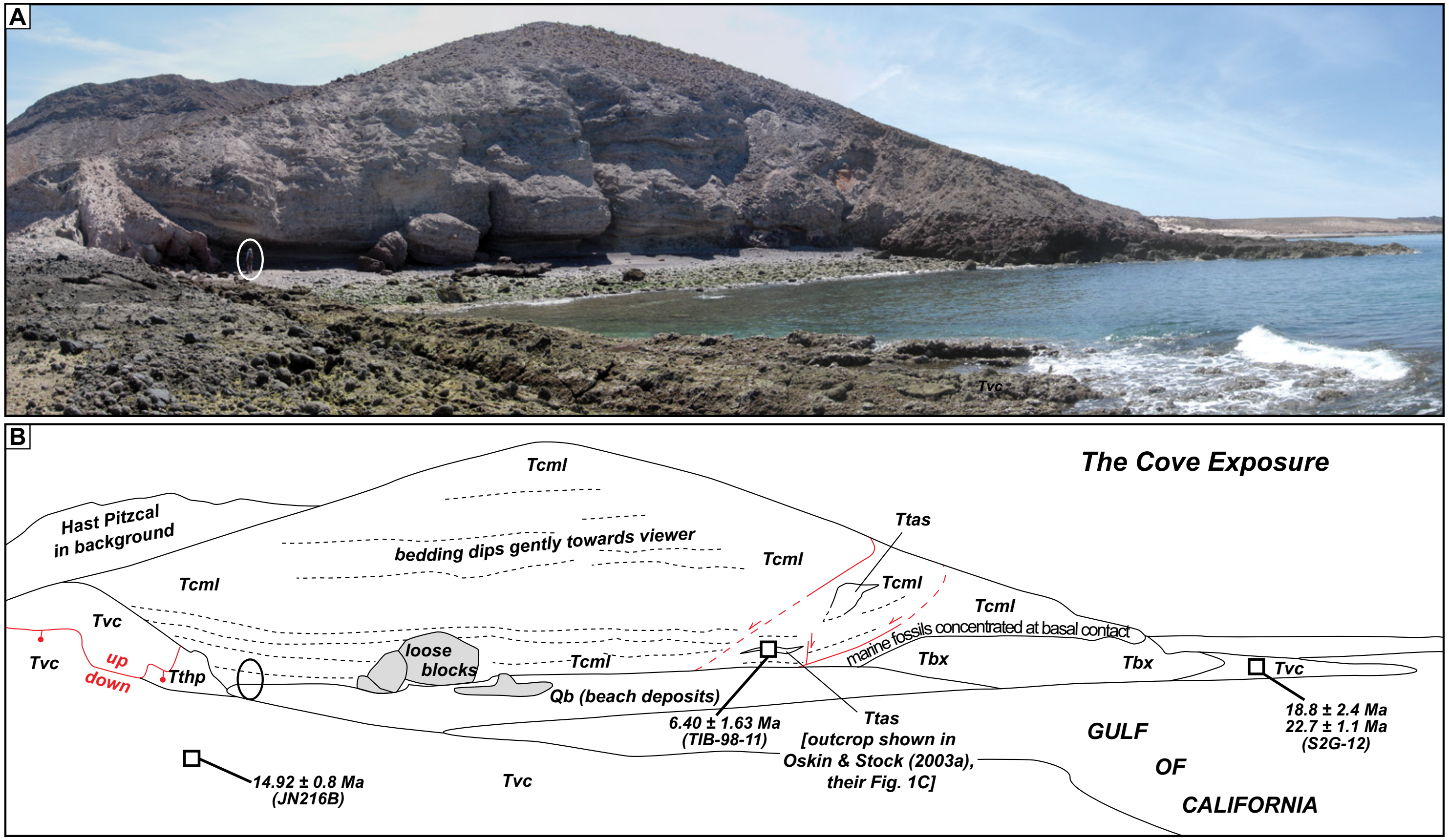

Figure 9. (A) Panoramic view of the cove outcrops where the floor of the marine basin is well exposed (circled person for scale). (B) Annotated interpretation of panorama in A. Marine conglomerate deposits (Tcml) containing discontinuous exposures of the tuff of Arroyo Sauzal (Ttas) unconformably overlie the landslide breccia (Tbx) and pre-basin volcaniclastic conglomerate (Tvc) (see text). Three previously published geochronologic ages have been reported from this cove outcrop. See geologic map (Fig. 2) for location and Supplemental Table 1 (see footnote 1) for details of units and ages.

Upper marine conglomerate and sandstone (Tcmu) is the most widespread sedimentary unit in the study area (Fig. 2). Tcmu overlies all older sedimentary and volcanic units (e.g., Tsmt, Tbx, Ttua, arc-related volcanic rocks) across a subhorizontal angular unconformity. Locally, in the northern part of the study area, the contact between Tcmu and underlying Tsmt and Tcmm appears conformable. Deposits of Tcmu consist of inclined beds of fossiliferous, pebble to cobble conglomerate (Fig. 11). Clasts of the 6.4 Ma tuffs of Mesa Cuadrada are rare in Tcmu (Oskin and Stock, 2003a). Tcmu appears to have been deposited by subaqueous sediment gravity flows (Cassidy, 1990; Oskin and Stock, 2003a). Its beds consistently dip ~15°–30° (typically ~25°) to the north or northwest. No microfossils were previously found in samples of Tcmu (Cassidy, 1990; Gastil et al., 1999). Common to abundant macrofossils are present, including oysters, pectens, barnacles, gastropods, echinoid spines and fragments, and small corals (Cassidy, 1990; Gastil et al., 1999; this study). Fossils typically are broken and rounded due to sedimentary transport.

Bedding dips in Tcmu are interpreted to be a primary dip acquired during deposition on a steep subaqueous slope in marine foresets of a Gilbert-type fan delta system. Gilbert-type fan deltas commonly form on steep margins of fault-bounded sedimentary basins by rapid deposition of coarse gravel and sand where alluvial fans deliver sediment directly into a standing body

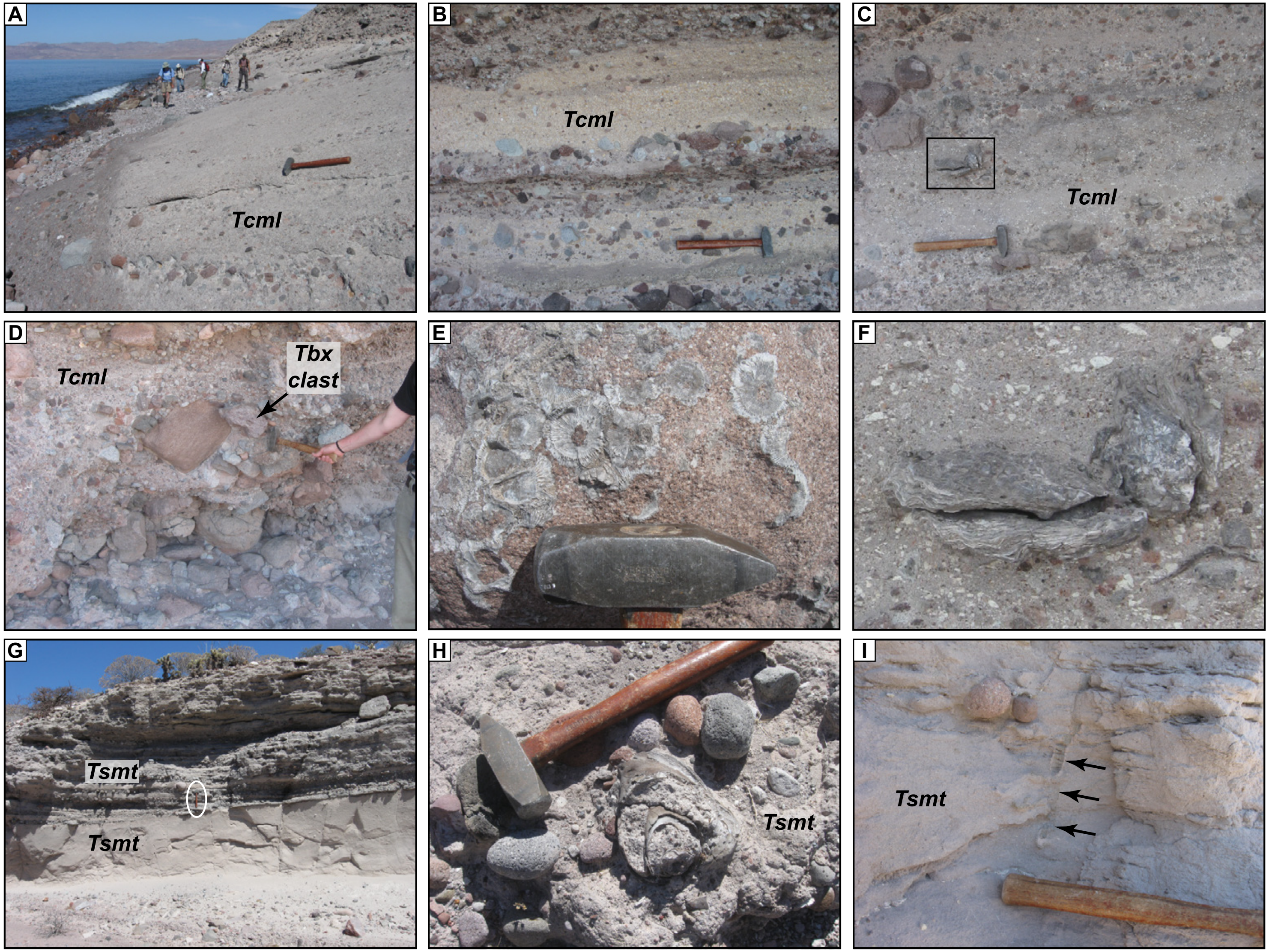

Figure 10. Field photographs of marine deposits on southwest Isla Tiburón. Hammer in each photo is 38 cm long (12.5-cm-wide hammer head). (A) Moderately to well-stratified lower conglomerate (Tcml) outcrops along coastline, northwest of Hast Pitzcal. (B) Well-stratified lower conglomerate (Tcml) outcrops in the cove (Fig. 9). (C) Fossiliferous lower conglomerate (Tcml) outcrops on the western flank of Hast Pitzcal. Black rectangle shows enlargement in F. (D) Poorly stratified lower conglomerate (Tcml) outcrops on the western bank of arroyo 2. Clast composition is dominated by locally derived arc-related volcanic rocks with occasional clasts of the distinctive landslide breccia deposit (Tbx). (E) Boulder in lower conglomerate (Tcml) encrusted with possible remnants of late Miocene barnacles. (F) Enlargement of rectangle area in C showing a pair of oyster fossils. (G) Outcrop of tuffaceous marine sandstone (Tsmt) deposits on the eastern bank of arroyo 2. Lower massive bed contains occasional layers of conglomerate stringers and marine fossils. Upper, well-stratified part contains fossiliferous sandstone and sandy conglomerate beds. (Hammer is circled.) (H) Large late Miocene gastropod fossil in Tsmt conglomerate bed. (I) Subvertical burrow (arrows) in tectonically inclined Tsmt sandstone and conglomerate beds.

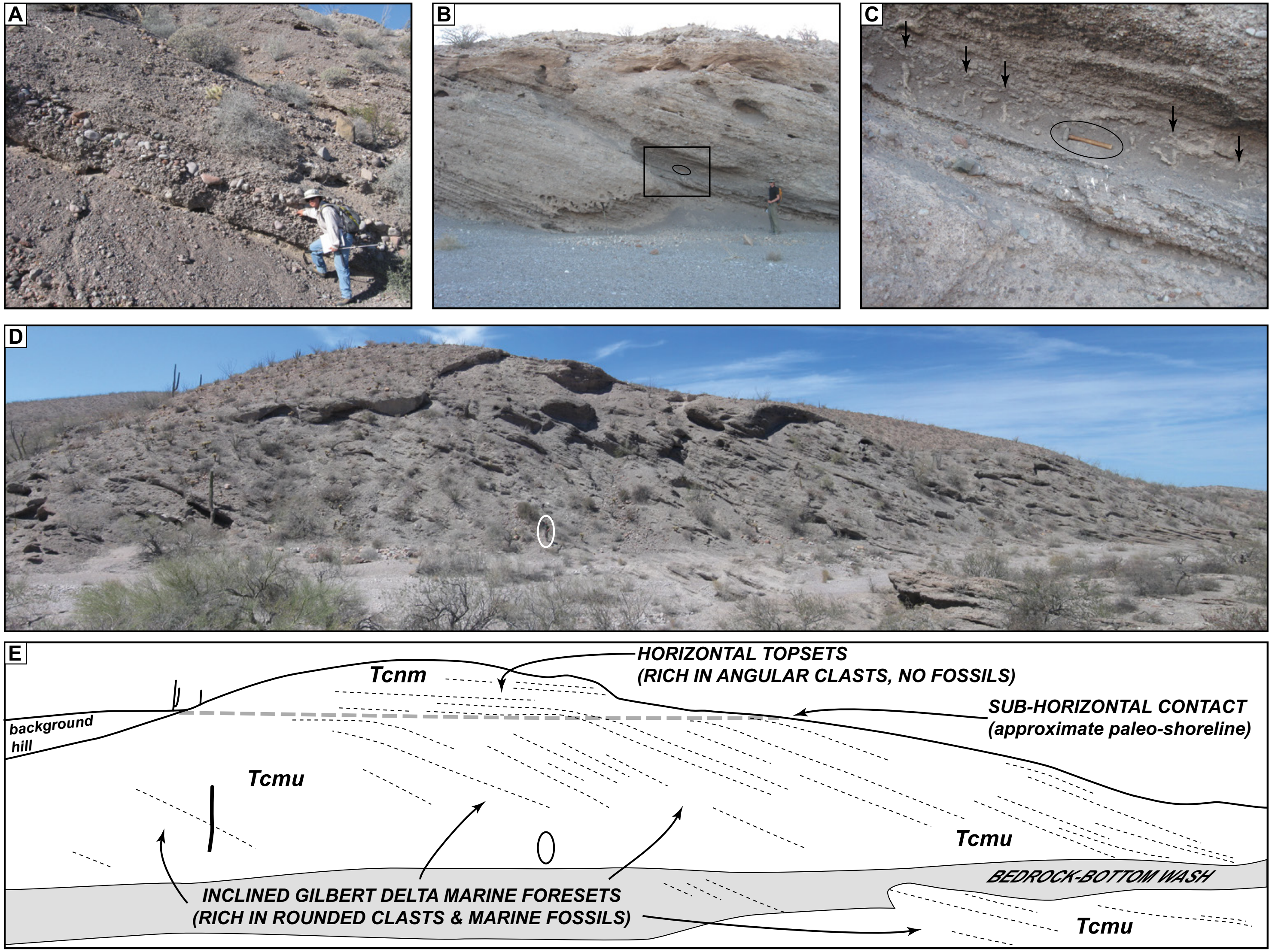

Figure 11. Field photographs of upper conglomerate (Tcmu) on southwest Isla Tiburón. Hammer for scale in B and C is 38 cm long. (A) An inverse graded Tcmu conglomerate bed on the western bank of arroyo 4. Bed inclination is primary depositional dip. (B) Inclined Tcmu conglomerate beds on the western bank of arroyo 4 containing multiple trace fossils. Black rectangle shows enlargement in C. (C) Enlargement of rectangle area in B showing multiple burrows in Tcmu sandy conglomerate bed. Subvertical burrows (black arrows) are oriented orthogonal to modern-day horizontal, not orthogonal to bedding. This supports that the ~25° inclination in Tcmu beds is due to primary depositional dip, and not tectonic tilting. (D) Panoramic view of Tcnm (nonmarine conglomerate and sandstone deposits) and Tcmu outcrops in arroyo 4. Looking west at exposure where subhorizontal, nonmarine topset beds (Tcnm) laterally grade into inclined, marine foreset beds (Tcmu). Circled person for scale. (E) Annotated interpretation of panorama in D.

of water (e.g., Gilbert, 1885; Gawthorpe and Colella, 1990; Postma, 1990; Falk and Dorsey, 1998; Ford et al., 2009). Vertical burrows observed in inclined beds (Figs. 11B, 11C) are consistent with this nontectonic interpretation for bedding dips in Tcmu.

The thickness of Tcmu was greatly overestimated (~1500 m) by Cassidy (1990) and Gastil et al. (1999), who interpreted that Tcmu beds were deposited subhorizontally in a subaqueous delta-fan system and subsequently tilted ~15°–30°. We disagree with their interpretation for the origin of the bedding dip, and instead estimate the thicknesses of Tcmu by measuring vertically through the undeformed foreset sequence, perpendicular to bounding topset strata and oblique to bedding dip in Tcmu. Tcmu is ~26 m thick in arroyo 4 (Keogh, 2010) near the southeastern edge of the marine deposits, and likely has a similar thickness along strike to the west-northwest. However, Tcmu thickens to the north, where we mapped an ~40-m-high hill between arroyo 3 and arroyo 4 entirely as Tcmu (Fig. 2). Gilbert-type fan delta systems of comparable thickness have been documented elsewhere in the Gulf of California (e.g., Dorsey et al., 1995; Umhoefer et al., 2007).

Nonmarine conglomerate and sandstone deposits (Tcnm) overlie all aforementioned sedimentary and volcanic Miocene units (Fig. 2). Tcnm (Figs. 12A, 12B) is mapped at higher elevation than marine deposits, and is located at the tops of many hills near arroyos 2, 3, and 4 (Fig. 2). Tcnm is observed near the top of Hast Pitzcal, stratigraphically beneath a capping lava flow (Fig. 2). The northeastern margin of the SWIT basin is mapped on the northeast side of arroyo 5, where Tcnm deposits are perched in buttress unconformity contact on the flanks of higher elevation hills of arc-related volcanic rocks (Figs. 12C, 12D). Nearby, two small west-draining paleotributaries are incised into older arc-related volcanic rocks and filled with Tcnm deposits, illustrating the form of the SWIT basin (Fig. 2).

Capping and Crosscutting Volcanic Rocks (Tthm, Tcsf, Tcsp, Tcsd)

The tuffs of Hipat Mesa (Tthm) are slightly welded, pumice-rich tuffs exposed near the modern shoreline (Fig. 2). Discontinuous exposures of Tthm between arroyos 4 and 6 overlie upper marine conglomerate and sandstone (Tcmu). Deposits of nonmarine conglomerate and sandstone (Tcnm) appear to project beneath Tthm outcrops between arroyos 5 and 6, although these units are not observed in contact with one another (Fig. 2). Zircons separated from a sample of Tthm yield a U/Pb age of 4.34 ± 0.20 Ma (Fig. 5C; Supplemental Table 2 [see footnote 2]). We correlate Tthm in the SWIT study area to more extensive and thicker tuff deposits capping Hipat Mesa, located 2–5 km southeast of the SWIT study area.

Our observations confirm that the rhyodacite of Cerro Starship (Tcsf) is a lava flow that was emplaced subaerially and caps all the marine and nonmarine strata of the SWIT basin. The lava flow forms a topographically prominent north-northeast–trending elongate hill, Hast Pitzcal (Figs. 13A and 14A). Tcsf is underlain by a thin, discontinuous, pumice-rich pyroclastic unit (Tcsp) (Fig. 13B). Along the elongate Hast Pitzcal exposure, the basal Tcsf contact dips gently northward (Fig. 13A), similar to the underlying subhorizontal nonmarine deposits. The top of the flow is a continuous, weathered, undulatory surface that also dips gently northward (Fig. 13C). At the outcrop scale, the flow deposit exhibits irregular centimeter-scale foliation (Fig. 13D) that rolls over from subhorizontal to subvertical across 5–10 m (Fig. 13E), indicating viscous flow.

We collected a sample from the basal vitrophyre of the main flow deposit (Fig. 2). Zircons separated from this sample yield a U/Pb age of 4.13 ± 0.09 Ma (Fig. 5D; Supplemental Table 2 [see footnote 2]). Analysis of the glass matrix from the same sample yields an Ar/Ar isochron age of 3.51 ± 0.05 Ma (Fig. 7B; Supplemental Table 4[4]). The Ar/Ar isochron age may provide a better estimate of the true eruption age than the U/Pb age (Simon et al., 2008). Both of these ages are consistent with a 4.16 ± 1.81 Ma (K-Ar) age that Neuhaus (1989) reported for a sample from the top of this flow. Gastil and Krummenacher (1977b) reported an 11.2 ± 1.3 Ma (K-Ar) age from this rhyodacite flow. This age is incongruent with other ages for Tcsf, and this flow being stratigraphically above in-place late Miocene sedimentary and volcanic units of the SWIT basin.

Parallel to and beneath the flow deposits of the rhyodacite of Cerro Starship (Tcsf) and its basal pyroclastic unit (Tcsp) is a system of subvertical, discontinuous dikes that extend beyond the north-northeast and south-southwest ends of Hast Pitzcal (Fig. 2). These dikes (Tcsd) are rhyodacite in composition and display a pervasive subvertical foliation (Fig. 13F). Gastil and Krummenacher (1977b) reported a 3.7 ± 0.9 Ma (K-Ar) age from an exposure of this dike on the east side of arroyo 1. South of the mapped Tcsf flow, discontinuous, north-northeast–striking, steeply east-southeast–dipping en echelon Tcsd dikes continue to the southern shoreline of Isla Tiburón (Figs. 2 and 13G).

Quaternary Sedimentary Deposits

Two generations of nonmarine, alluvial to fluvial conglomerate and sandstone deposits of presumed Quaternary age are found on flat, low-lying terraces as much as 110 m above modern sea level (Fig. 2). The basal contact of these terraces is subhorizontal, and dips gently toward the Gulf of California, similar to its dissected upper geomorphic surfaces. Remnants of an older generation of alluvial terraces (Qoa2) are preserved within 1–2 km of the coastline, near the mouths of arroyos 4, 5, and 6. A more extensive, younger generation of alluvial terraces (Qoa) is observed in arroyos throughout the study area, perched as much as ~10 m above the active channels (Fig. 2). Thin benches of recent marine terraces (Qmt) are perched ~5–10 m above modern sea level. Between arroyos 2 and 5, subtle geomorphic evidence exists for a recent wavecut bench at ~8 m elevation, ~150 m inland from the modern shoreline. These marine deposits are likely coeval with the more extensive nonmarine alluvial deposits (Qoa, Qoa2) and could be related to a global sea-level highstand during a Pleistocene interglacial period (marine isotope stage 5e) (Ortlieb, 1991) or earlier. It is plausible that in some places the marine-nonmarine transition between Qmt and Qoa-Qoa2 is farther inland, and some of the deposits mapped

Table 4. $^{40}Ar/^{39}Ar$ step-heating data of volcanic matrix from the Rhyodacite of Cerro Starship, Southwest Isla Tiburón, México.

Step	Temp. °C	% ^{39}Ar of total	Radiogenic Yield (%)	$^{39}Ar_k$ (moles x 10^{-12})	$^{40}Ar^*/^{39}Ar_k$	Apparent K/Ca	Apparent K/Cl	Apparent Age (Ma)	Error (Ma)
TIB-09-06	***dacite matrix***	*J = 0.004439 ± 0.30%*		*wt = 356.1 mg*	*#187&188KD53*				
A	550	1.9	5.5	0.0007	0.393	4.95	71	3.14	± 0.12
B	600	1.3	24.6	0.0131	0.426	5.88	99	3.41	± 0.11
C	700	7.2	51.0	0.0176	0.413	6.03	109	3.31	± 0.02
D	800	14.5	72.6	0.0281	0.421	5.00	108	3.36	± 0.01
E	900	23.6	76.4	0.0338	0.434	3.14	105	3.47	± 0.01
F	1000	29.9	71.6	0.0227	0.445	1.87	105	3.56	± 0.01
G	1100	18.5	62.0	0.0044	0.457	1.31	107	3.65	± 0.01
H	1200	2.3	44.5	0.0007	0.457	0.39	100	3.65	± 0.08
I	1300	0.5	21.4	0.0003	0.426	0.11	28	3.41	± 0.33
J	1450	0.4	17.4	0.0003	0.396	0.07	59	3.17	± 0.57
Total Gas		100	66.7	0.1216	0.438	3.09	105	3.5	

Ages calculated assuming an initial $^{40}Ar/^{36}Ar = 295.5 \pm 0$
All precision estimates are at the one sigma level of precision.
Ages of individual steps do not include error in the irradiation parameter J.
No error is calculated for the total gas age.

[4]Supplemental Table 4. $^{40}Ar/^{39}Ar$ step-heating data of volcanic matrix from the Rhyodacite of Cerro Starship, Southwest Isla Tiburón, México. Please visit http://dx.doi.org/10.1130/GES01153.S4 or the full-text article on www.gsapubs.org to view Supplemental Table 4

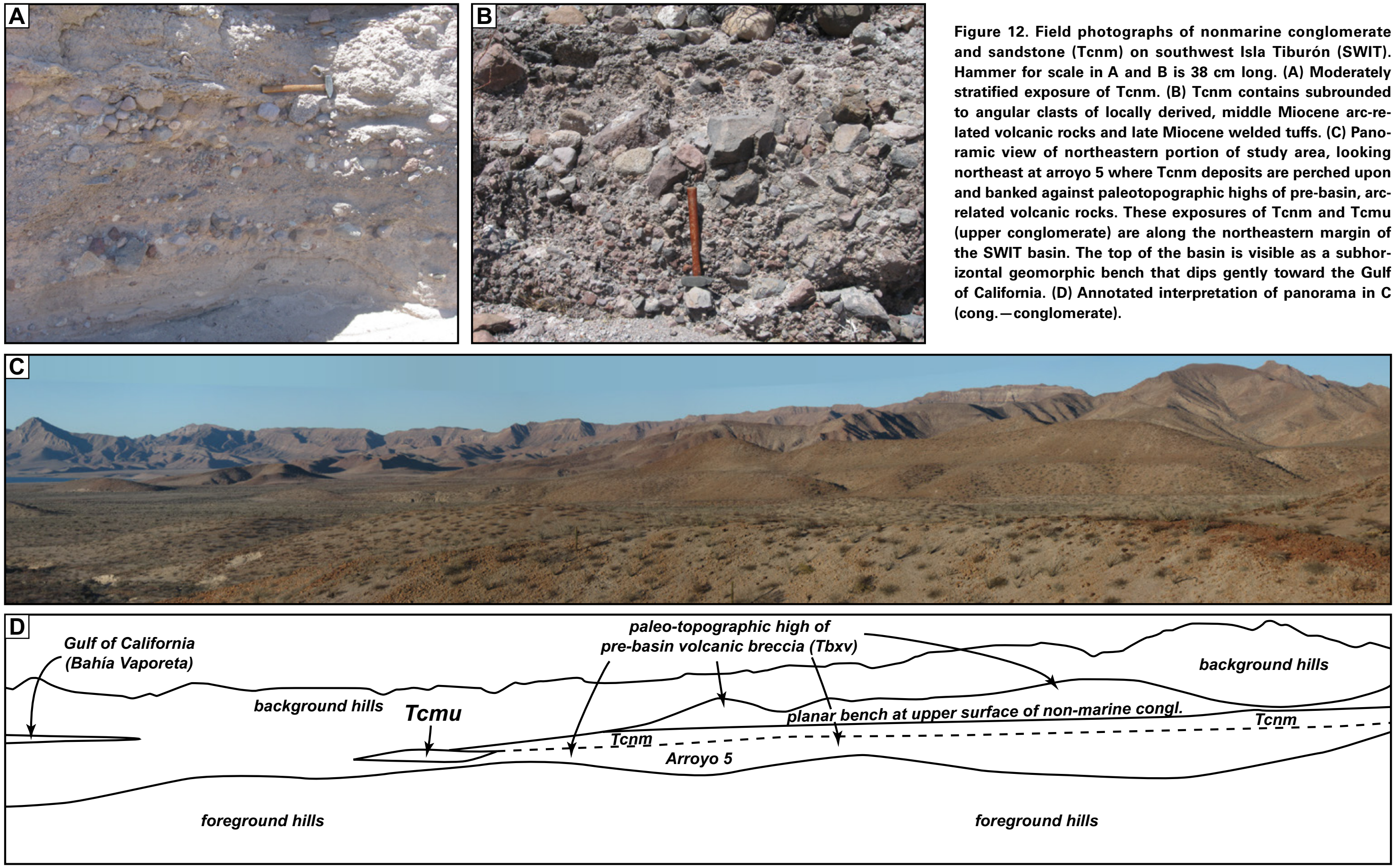

Figure 12. Field photographs of nonmarine conglomerate and sandstone (Tcnm) on southwest Isla Tiburón (SWIT). Hammer for scale in A and B is 38 cm long. (A) Moderately stratified exposure of Tcnm. (B) Tcnm contains subrounded to angular clasts of locally derived, middle Miocene arc-related volcanic rocks and late Miocene welded tuffs. (C) Panoramic view of northeastern portion of study area, looking northeast at arroyo 5 where Tcnm deposits are perched upon and banked against paleotopographic highs of pre-basin, arc-related volcanic rocks. These exposures of Tcnm and Tcmu (upper conglomerate) are along the northeastern margin of the SWIT basin. The top of the basin is visible as a subhorizontal geomorphic bench that dips gently toward the Gulf of California. (D) Annotated interpretation of panorama in C (cong.—conglomerate).

as Qoa-Qoa2 near the modern-day shoreline are instead Qmt. Younger fluvial sand and cobble deposits (Qal) are found in active channels (arroyos 0–6). A strip of unconsolidated beach sand and cobble deposits (Qb) is found along the modern shoreline, and a veneer of unconsolidated eolian sand deposits (Qae) is found inland as much as 1.5 km from the modern shoreline.

Faults and Folds

Several structures associated with the La Cruz fault system deform rocks on SWIT. The intensity of deformation is greatest in the older marine units and underlying early to middle Miocene volcanic rocks. The uppermost marine rocks (Tcmu) and superadjacent nonmarine rocks (Tcnm) are only slightly deformed and overlie older, deformed strata across an angular unconformity. The capping Pliocene volcanic units and Quaternary sedimentary units appear to be undeformed.

The La Cruz fault is a major northwest-striking, dextral strike-slip fault that parallels the southwestern coastline of the island (Fig. 1B) and cuts most late Miocene and older map units on SWIT (Figs. 2, 14B, and 14C). Although the La Cruz fault is primarily a subvertical strike-slip fault, it also has a history of vertical offset, with evidence for both transpressional and transtensional deformation. Overall displacement across the fault in the study area is dextral oblique normal, with down-to-the-northeast vertical offset. Crystalline basement rocks are exposed southwest of the fault and are not exposed north-

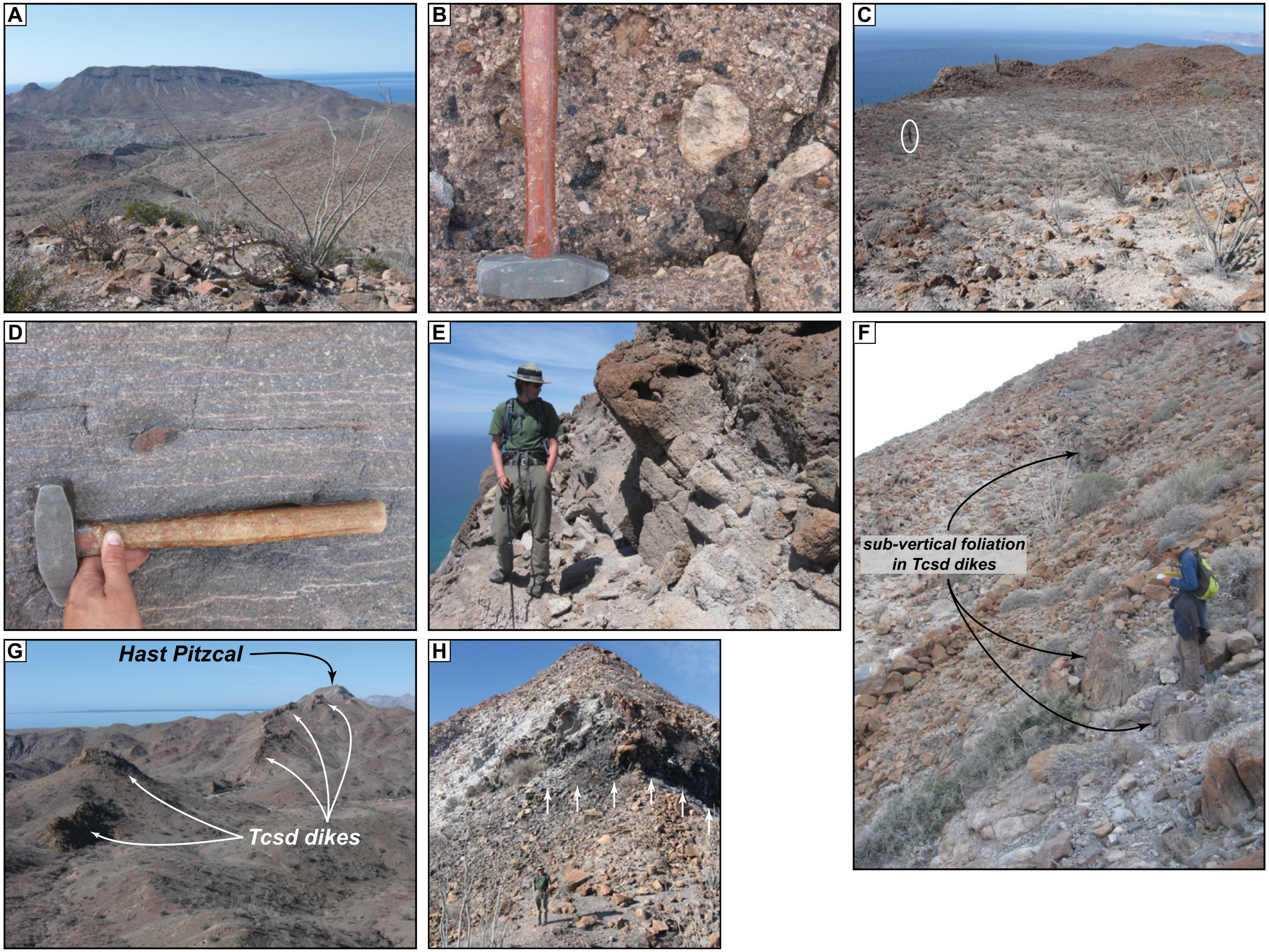

Figure 13. Field photographs of Hast Pitzcal (Cerro Starship) hill and Pliocene volcanic units that cap and cut through the marine basin on southwest Isla Tiburón. Hammer for scale in B and D is 38 cm long. (A) Looking northwest at Hast Pitzcal. Resistant hilltop is ~1 km in length. (B) Ash- and pumice-rich pyroclastic deposits (Tcsp) locally underlie the capping Rhyodacite of Cerro Starship (Tcsf) lava flow. (C) Looking north along undulatory upper surface of Hast Pitzcal. No crosscutting dikes are observed along crest of hilltop. Circled geologist for scale. (D) Centimeter-scale flow banding in porphyritic rhyodacite. Maroon object in center of photo is loose clast. (E) Flow banding in rhyodacite outcrops (Tcsf) shows highly variable patterns of foliation, suggesting viscous flow prior to cooling. (F) Looking southwest on the eastern flank of Hast Pitzcal at subvertical foliation in feeder dikes (Tcsd). Foliation in Tcsd is parallel to outcrop pattern of dike outcrops. Dike leads directly to base of capping Rhyodacite of Cerro Starship (Tcsf) lava flow. (G) Looking north from southwestern corner of study area. Discontinuous, en echelon rhyodacite dikes (Tcsd) lead to capping Rhyodacite of Cerro Starship (Tcsf) at Hast Pitzcal. (H) Looking north at southernmost tip of main flow body of Tcsf. Base of rhyodacite flow consists of 2–4-m-thick black glassy vitrophyre. Geologist is standing on middle Miocene arc-related basalt flows. Basal contact of Tcsf (white arrows) is continuous and sharp. No crosscutting dikes are observed. White region in upper left portion of photo is recent landslide scar.

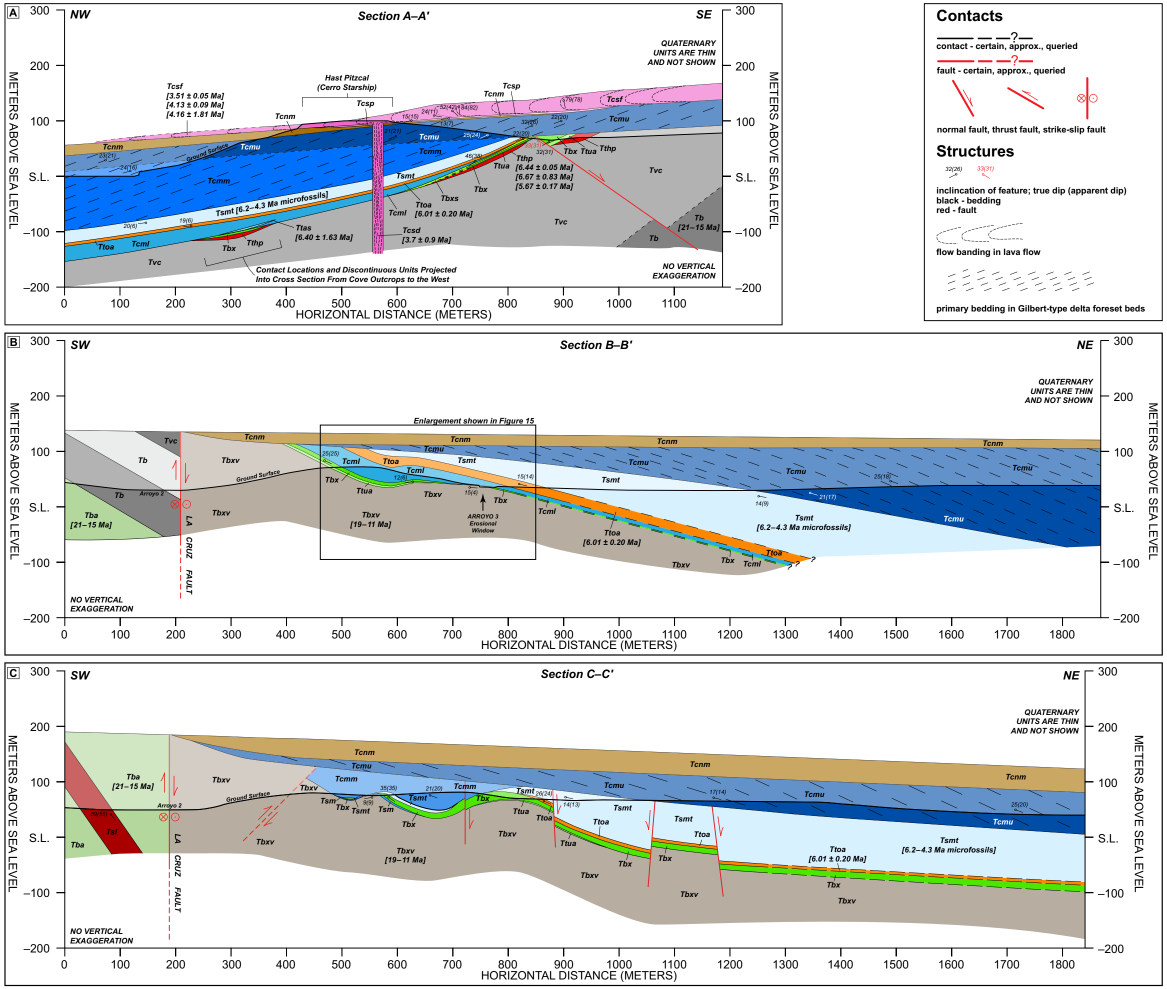

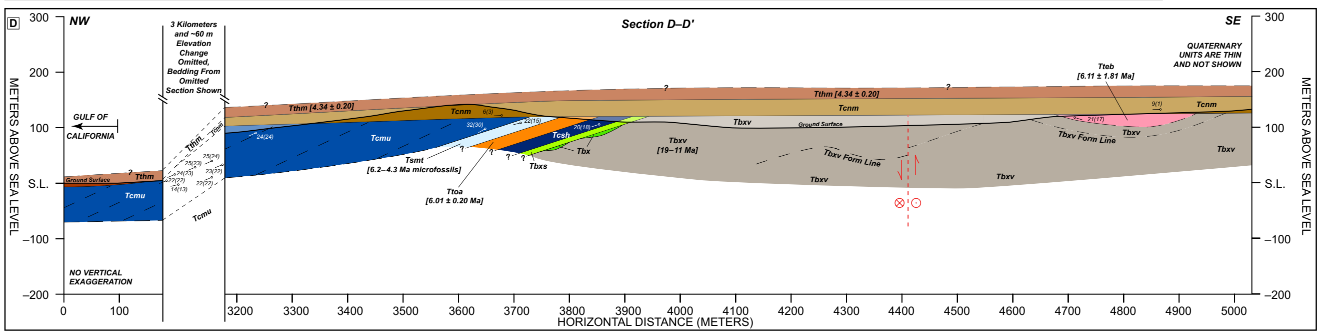

Figure 14. (A–D) Geologic cross sections for southwest Isla Tiburón. Map unit colors and other symbols as in Figure 2. S.L.—sea level. Units shaded lighter are above the ground surface. Dip values from structural measurements used to construct cross sections are shown near ground surface. Apparent dip values are in parentheses. Horizontal scale arbitrarily begins at 0 m at left edge of each cross section. See geologic map (Fig. 2) for cross-section line locations. To view the large-format map plate, please visit http://dx.doi.org/10.1130/GES01153.S3 or the full-text article on www.gsapubs.org. Printed cross-section sheet is 19″ tall, 19″ wide (~48 × 48 cm).

east of the fault in the study area (Fig. 2). The base of the marine section has ~1 km of dextral separation in arroyo 2 (Fig. 2). The La Cruz fault cuts unit Tsmt and all older marine and nonmarine units. Adjacent faults and folds do not appear to deform the La Cruz fault. From this we surmise that slip on these secondary structures was contemporaneous with slip on the La Cruz fault in a dextral-wrench shear zone.

The total dextral offset on the La Cruz fault is not well constrained, because none of the older, arc-related units match across its 28 km length across southern Isla Tiburón (Oskin and Stock, 2003a), suggesting that it may have undergone at least tens of kilometers of total dextral displacement. However, less dextral offset may be required if down-to-the-northeast displacement across the fault has obscured correlative units. Younger arc-related volcanic rocks northeast of the fault may conceal older arc-related units that are correlative to those now exposed southwest of the fault. Bennett (2013) suggested only 5 ± 2 km of dextral offset for the La Cruz fault, based on correlation of paleovalley exposures of the 12.5 Ma tuff of San Felipe across the fault ~10 km southeast of SWIT.

Many map units are also deformed by folds and reverse faults. Mapped folds are gentle, with ~120°–155° interlimb angles (Fig. 14). The traces of fold axial planes are oriented approximately west-northwest–east-southeast, slightly more westward than the northwest-striking La Cruz fault (Fig. 2). Reverse faults are oriented between northwest-southeast and east-west, and dip 20°–80° south to southwest. Displacement on these faults is minor, with tens to hundreds of meters of total slip. Folds and reverse faults only deform unit Tsmt and older units. In general, map units on both sides of the La Cruz fault dip north, except locally in south-dipping fold limbs. This is expressed on the geologic map (Fig. 2) as map units that are progressively younger from south to north.

Normal faults also are present in the study area (Figs. 2 and 14). Mapped normal faults are oriented approximately north-northwest to north-northeast with moderate to steep dips. Displacement on these normal faults is minor, with tens of meters of total displacement. Normal faults deform Tsmt and older units, and cut folds and reverse faults. The dike system (Tcsd) that fed the Rhyodacite of Cerro Starship (Tcsf) is oriented approximately north-northeast across SWIT, subparallel to the strike of many mapped normal faults in the study area (Fig. 2) and southeast of the study area across southern Isla Tiburón (Bennett, 2013). This orientation is similar to the expected orientation of extensional structures (e.g., fractures and faults) in the transtensional Gulf of California (Withjack and Jamison, 1986). The Tcsd dike system likely formed under a transtensional strain field.

Deformation associated with the La Cruz fault and adjacent faults and folds likely initiated sometime after the emplacement of the youngest arc-related volcanic rocks (ca. 11 Ma), and prior to the emplacement the pre-marine volcanic rocks (ca. 6.5 Ma) and subsidence of the SWIT basin. Activity on the La Cruz fault ~10 km southeast of SWIT commenced between 12 and 8 Ma (Bennett, 2013). Deformation was ongoing during sedimentation in the SWIT marine basin. The oldest marine units, Tsm, Tcml, and Tcsh, are faulted and folded in a manner similar to underlying arc-related volcanic rocks. Intermediate-age marine units Ttoa, Tsmt, and Tcmm are the youngest map units folded or cut by these faults. Younger units, including the Gilbert delta system foreset deposits (Tcmu) and laterally equivalent nonmarine conglomerate (Tcnm), appear to be undeformed and cap all faults in the SWIT study area (Fig. 2). We conclude that deformation associated with the La Cruz fault likely ceased sometime after emplacement of the 6.01 ± 0.20 Ma tuff of Oyster Amphitheater, around the time of emplacement of the 3.51 ± 0.05 Ma to 4.13 ± 0.09 Ma Rhyodacite of Cerro Starship and 4.34 ± 0.20 Ma tuffs of Hipat Mesa.

RESOLUTION OF SWIT CONTROVERSIES

The results of our new detailed geologic mapping, geochronology, and stratigraphic analysis support the interpretation that marine rocks on SWIT were deposited during latest Miocene to Pliocene time (Oskin and Stock, 2003a). Based on these results, we address and resolve long-standing controversies over the age and depositional setting of the SWIT marine basin and the age and emplacement mechanism of several volcanic units that provide key constraints on the timing of marine deposition.

Age of Marine Strata in the SWIT Basin

Smith et al. (1985) published a 12.9 ± 0.4 Ma age for a monolithologic andesite breccia (their sample 83BSJ260) that they interpreted to be interstratified with marine deposits near the base of the SWIT basinal section, in deposits of the white tuffaceous marine sandstone unit (Tsmt) (Smith, 1991). Oskin and Stock (2003a) suggested that this breccia outcrop belongs to older volcaniclastic strata stratigraphically below the marine deposits but their mapping was insufficient to verify this notion. An enlargement of our cross-section B-B′ illustrates the structural and stratigraphic relationship of this exposure to the unconformably overlying marine deposits (Fig. 15). The andesite breccia sample locality (Fig. 4C) is located in the bedrock floor of arroyo 3 (Fig. 15, 750 m on horizontal distance scale), which is surrounded by higher topography. On the hill south of the arroyo exposure, Tcml, Tbx, and older units are all deformed by gentle folds (Fig. 15). A gently north-dipping fold limb is mapped on the north-facing dip slope of this hill, with beds dipping toward the arroyo exposure. The sharp, ~15° north-dipping basal contact of marine conglomerate (Tcml) is exposed 1–2 m above the arroyo bottom on the northeastern and southwestern sides of the ~20-m-wide bedrock-bottom arroyo (Fig. 15). In the arroyo floor, the distinctive landslide breccia (Tbx) is in contact stratigraphically above the andesitic breccia (Tbxv), and nearby, is stratigraphically below the marine conglomerate. Thus, as suggested in Oskin and Stock (2003a), the andesite breccia at this location is exposed in an erosional window carved through and surrounded by gently dipping marine conglomerate and landslide breccia that unconformably overlie the andesite breccia (Fig. 15). In fact,

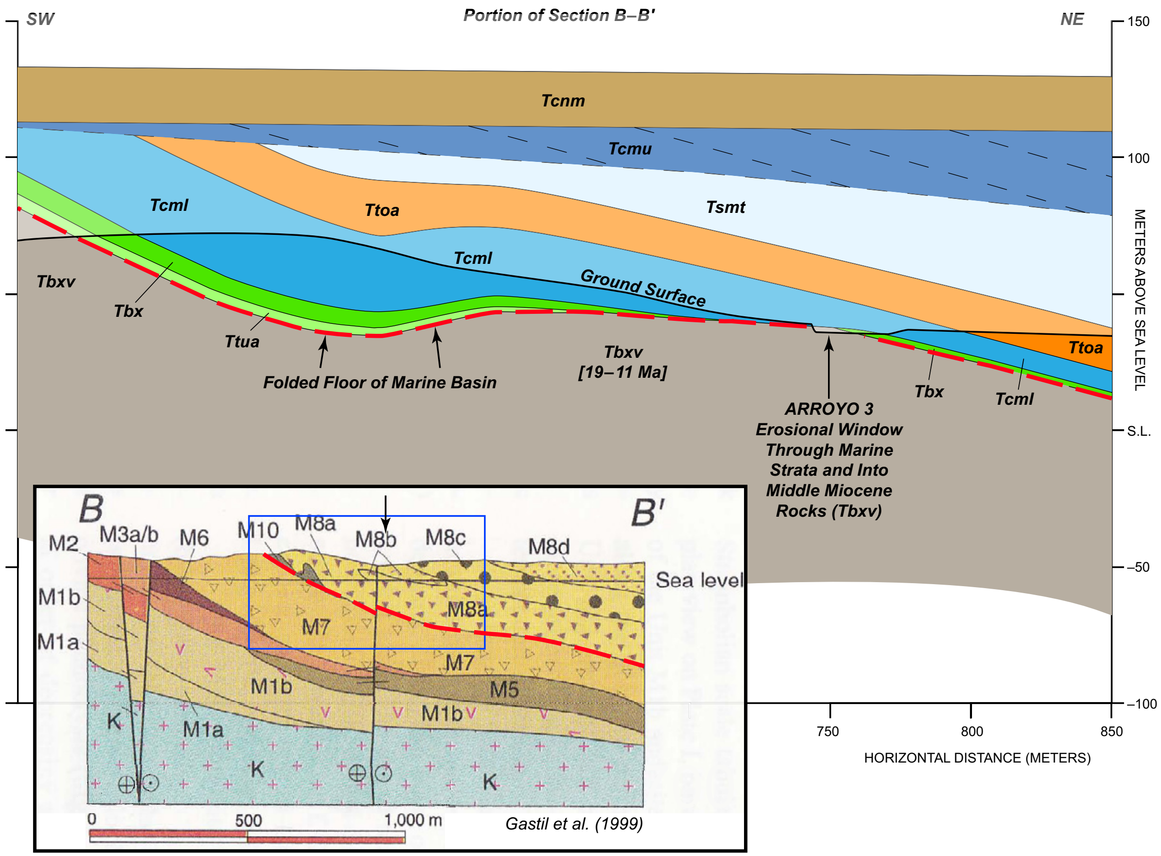

Figure 15. Cross section of erosional window exposure in arroyo 3 where Smith et al. (1985) collected and dated (12.9 ± 0.4 Ma; K-Ar) a sample of andesitic breccia, thought to be interbedded in marine strata. This figure is an enlargement of a portion of our cross-section B-B′ (Fig. 14B). Lower left inset shows cross-section B-B′ by Gastil et al. (1999), drawn along same line as our cross-section B-B′ (note different scale). Extent of main enlargement is indicated by blue rectangle in inset. Gastil et al. (1999) showed unit M8b, the unit that Smith et al. (1985) dated, as a discontinuous, fault-bounded wedge of andesite interbedded within marine strata (e.g., M8a, M8c, M8d). We map this unit as Tbxv (see text). The floor of the marine basin is highlighted by a red dashed line on both cross sections. Our detailed mapping demonstrates that arroyo 3 exposes an erosional window through the folded floor of the marine basin and into older arc-related volcanic rocks (Tbxv) and the landslide breccia (Tbx). M1–M7 of Gastil et al. (1999) is equivalent to our arc-related volcanic rocks (e.g., Tbxv, Tbxd). M10 is equivalent to our landslide breccia (Tbx), interpreted by Gastil et al. (1999) as a younger, cross-cutting rhyolite dike.

we mapped multiple erosional windows such as this within 0.5 km of this key outcrop (Fig. 2). These relationships demonstrate that the isotopically dated andesitic breccia is stratigraphically below, rather than within, the marine deposits and is part of the older arc-related volcanic rocks (Tbxv).

In this study we provide new age constraints that bracket the marine deposits on SWIT. The lithologically distinctive landslide breccia marker (Tbx) is exposed almost continuously at the base of the marine section. In general, this breccia directly overlies, in angular unconformity, pre-marine, early rift volcanic rocks (e.g., Tthp) or early to middle Miocene arc-related volcanic rocks (e.g., Tbxv). At some locations, however, it overlies a thin (<5 m) discontinuous unit of marine sandstone (Tsm) that in turn overlies arc-related volcanic rocks. The age of this distinctive marker unit, and thus the base of the marine deposits, is bracketed between the 6.44 ± 0.05 Ma tuff of Hast Pitzcal that underlies the marine section, and the 6.01 ± 0.20 Ma tuff of Oyster Amphitheater, which is interbedded within the basal marine deposits. The youngest SWIT marine deposits predate emplacement of the 3.51 ± 0.05 Ma to 4.13 ± 0.09 Ma rhyodacite of Cerro Starship and the 4.34 ± 0.20 Ma tuffs of Hipat Mesa.

A latest Miocene to Pliocene age for the SWIT marine basin was previously indicated by the presence of 6.2–4.3 Ma marine microfossils described by Gastil et al. (1999). However, this biostratigraphic age constraint was not incorporated into the conclusions of the original study (Gastil et al., 1999) and it has been ignored in subsequent paleontological studies in the Gulf of California. Carreño and Smith (2007) and Helenes et al. (2009) asserted that the SWIT marine basin is middle Miocene in age, referring to the 12.9 ± 0.4 Ma age interpretation of Smith et al. (1985) and the 11.2 ± 1.3 Ma age of Gastil and Krummenacher (1977b) for the rhyodacite flow that caps the marine basin, despite doubts raised about these constraints in Oskin and Stock (2003a). Helenes et al. (2009) cited the late Miocene microfossils of Gastil et al. (1999)

as evidence for a younger marine incursion that they interpreted to be distinct and younger than their inferred middle Miocene seaway. That interpretation is untenable because it assumes a middle Miocene age for the base of the marine section on SWIT, which we show here is incorrect. The results of our study agree with previously published biostratigraphic evidence for a latest Miocene to early Pliocene age of earliest marine sedimentation and conclusively resolve previous age controversies for the SWIT basin.

Of more regional concern, paleontological studies of molluscan assemblages (e.g., Smith et al., 1985; Smith, 1991; Carreño and Smith, 2007) have used the fossil assemblage from SWIT as a megafossil standard for middle Miocene time in the Gulf of California, thus influencing age interpretations of marine basin deposits at other locations. These paleontological studies incorrectly assigned a middle Miocene age to similar megafossil assemblages over a significant length of the Gulf of California and Salton Trough, including the Imperial Formation >650 km northwest of Isla Tiburón, the basal Boleo Formation >150 km south of Isla Tiburón, and the basal Trinidad Formation >650 km southeast of Isla Tiburón (Gastil et al., 1999). Marine deposits at some of these locations have subsequently been shown to be late Miocene in age (e.g., McDougall et al., 1999; Dorsey et al., 2007, 2011). Future paleontological studies in the Gulf of California region should discontinue use of the erroneous middle Miocene interpretation for the age of marine strata and fossil assemblages on SWIT.

Depositional Setting of the SWIT Basin

Our detailed structural and stratigraphic results require a reinterpretation of the controls on SWIT basin geometry, subsidence, and depositional setting. Most of the subsidence that formed the SWIT basin took place northeast of the La Cruz fault in response to down-to-the-northeast separation. The exposed marine deposits fill an elongate, 1.5–2.5-km-wide trough for 4 km parallel to the fault trace (Fig. 2). This trough continues to the southeast for at least an additional 5 km, and is occupied by nonmarine strata that we infer to be laterally equivalent to the marine section (Fig. 1B; Bennett, 2013). For most of its length, the basin is restricted to the northeast side of the La Cruz fault, supporting the idea that it formed above the down-dropped, northeastern side of this dextral oblique fault zone. Within ~1 km of the modern shoreline, the outcrop belt of sedimentary rocks widens to >4 km and latest Miocene to Pliocene marine deposits are preserved on both sides of the La Cruz fault.

We interpret the map units Tsmt, Tcmm, Tcmu, and Tcnm to represent a linked fluvial-marine Gilbert-type fan delta system (e.g., Gilbert, 1885; Gawthorpe and Colella, 1990; Postma, 1990; Falk and Dorsey, 1998; Ford et al., 2009) fed by a northwest-flowing fluvial system that drained watersheds across much of southern Isla Tiburón and delivered coarse gravelly sediment to the late Miocene Gulf of California seaway. The transport direction and architecture of the Gilbert-delta system was controlled by the latest stages of deformation on the La Cruz fault; only the lower units of the delta deposits (e.g., Tsmt, Tcmm) are folded or faulted. Nonmarine topset deposits (Tcnm) both truncate (Figs. 11D, 11E; see also Fig. 1D of Oskin and Stock, 2003a) and pass laterally in the transport direction into inclined marine foreset deposits (Tcmu) (Figs. 11D, 11E). Gently dipping marine tuffaceous sandstone deposits (Tsmt) are interpreted to be marine turbidites formed in distal Gilbert-delta bottomsets. In places, coarser marine conglomerate and sandstone (Tcmm) erosionally overlie Tsmt, possibly recording a temporary fall in relative sea level. Marine conglomerate deposits (Tcmu) overlie Tsmt and Tcmm. We interpret Tcmu as a system of prograding marine foresets. Sediments were sourced from an updip fluvial system to the southeast, and prograded to the northwest across older, deformed marine units (e.g., Tsm, Tcml). The fan delta deposits appear to have filled a marine embayment that formed as a result of subsidence along the La Cruz fault in an area that previously hosted a more heterogeneous, isolated set of fault-bounded marine subbasins.

We estimate that marine deposits of SWIT have a total maximum thickness of ~300 m in the study area, based on a combination of our detailed geologic mapping and compilation of detailed measured sections (Keogh, 2010). This estimate utilizes maximum thickness measurements of ~10 m of Tsm, Ttua, and Tbx, ~130 m of Tbxs, Tcml, and Tcsh, ~30 m of Ttoa, ~90 m of Tsmt, ~100 m of Tcmm, ~40 m of Tcmu, and ~50 m of Tcnm. However, marine units are of variable thickness across the study area and in no single section are all observed at their maximum thickness. Our basin thickness estimate is significantly less than the ~1500 m estimate of Cassidy (1990) and Gastil et al. (1999), who incorrectly calculated thickness for the Tcmu unit of the Gilbert-type fan delta system, for which bed inclination is nontectonic.

Reinterpretation of Late Miocene Igneous Units

Neuhaus (1989) and Gastil et al. (1999) mapped and dated three late Miocene igneous units interpreted as dikes or pods of rhyolite flows that crosscut and/or overlie all SWIT marine deposits (Fig. 2; Supplemental Table 1 [see footnote 1]). Our observations indicate that none of these igneous units crosscut or overlie marine strata, but rather are within the stratigraphic section, where they are faulted and folded similar to underlying and overlying map units.

A rhyolite from arroyo 1 was interpreted as either a flow that overlies SWIT marine conglomerate (Neuhaus, 1989; unit Mr) or as a crosscutting dike (Gastil et al., 1999; unit M10). Their petrographic descriptions are very similar to our description of the tuff of Hast Pitzcal (Tthp), which crops out at their sample location on our geologic map (Fig. 2). The previous K-Ar age of 5.67 ± 0.17 Ma from the west side of arroyo 1 (Neuhaus, 1989) is broadly similar to our Ar/Ar age of 6.44 ± 0.05 Ma for Tthp, from the opposite site of the arroyo. In this area, Tthp is tilted and faulted and unequivocally within the stratigraphic section, unconformably beneath marine deposits (Figs. 2 and 14A). Locally, in a side canyon on the western side of arroyo 1, the upper contact of Tthp diapirically intrudes overlying stratified ash and pumice beds of unit Ttua (Fig. 6). We observe similar diapiric relationships in outcrops just west of a coastal cove, between arroyo 0 and Hast Pitzcal (Fig. 2). This contact relationship may have occurred as a result of the rapid deposition and overburden pressure of these breccia deposits onto older, unconsolidated deposits of water-saturated tuff. Such local diapric flow contact relationships may have led to previous interpretations that the emplacement of the tuff of Hast Pitzcal occurred as an intrusion.

Neuhaus (1989) mapped another local rhyolite unit (Mry) from an outcrop in arroyo 4, in the southeastern corner of the study area (Fig. 2) and reported a 6.11 ± 1.81 Ma (K-Ar) age for this unit (Supplemental Table 1 [see footnote 1]). Neuhaus (1989) interpreted this unit as a rhyolite flow that overlies SWIT marine conglomerate. Gastil et al. (1999) also reported this age, but located this volcanic sample among outcrops of fluvial conglomerate (M11) on their geologic map. The sample location and petrographic description of Neuhaus (1989) are both similar to the tuff of Ensenada Blanca (Tteb) on our geologic map (Fig. 2), where Tteb is deposited upon older arc-related volcanic breccia deposits (Tbxv) and is not in contact with marine strata (Fig. 14D). Because Tteb is overlain by nonmarine conglomerate (Tcnm), a unit coeval with the youngest SWIT marine deposits (Tcmu), and is gently folded similar to the oldest marine deposits (Tcml), Tteb is likely to predate or be coeval with marine conditions on SWIT.

Gastil et al. (1999) mapped a discontinuous rhyolite unit (M10) in the vicinity of arroyos 1, 2, and 3, from which a 9.02 ± 1.18 Ma (Ar/Ar) age was obtained. They interpreted this unit as a rhyolite dike crosscutting marine conglomerate. Our mapping indicates that these outcrops are moderately dipping deposits of the distinctive landslide breccia unit (Tbx) (Fig. 2), which consists predominantly of welded rhyolite tuff clasts (Figs. 8A, 8B), and was emplaced near the base of the marine rocks (Fig. 14B). Breccia clasts of Tbx are identical to primary tuff outcrops of tuff of Ensenada Blanca (Tteb). We also observe angular to subrounded cobbles and boulders of cemented Tbx reworked into overlying Tcml marine conglomerate beds (Figs. 2 and 10D) that further confirm that it predates most marine sediments. If we take the ages from these units reported by Gastil et al. (1999) at face value, these data suggest that the tuff of Ensenada Blanca, which provided the source of clasts within Tbx, was likely emplaced ca. 9–7 Ma, prior to marine conditions on SWIT.

Age and Emplacement of the Rhyodacite of Cerro Starship

Conflicting interpretations (Gastil and Krummenacher, 1977b; Gastil et al., 1999; Oskin and Stock, 2003a) have been suggested for the age and emplacement mechanism of the rhyodacite of Cerro Starship (Tcsf), which caps all marine deposits (Fig. 13). The basis for this conflict is in the disparity between the original K-Ar ages obtained by Gastil and Krummenacher (1977b) for the flow (11.2 ± 1.3 Ma) versus a nearby dike of similar lithology (3.7 ± 0.9 Ma), leading to their interpretation that these features are separate igneous events. A younger K-Ar age of 4.16 ± 1.81 Ma for a sample collected from the top of the flow by Neuhaus (1989) and reported in Gastil et al. (1999) was interpreted to have been accidentally collected from a younger, crosscutting dike instead. This interpretation was rejected in Oskin and Stock (2003a) and it was instead proposed that the K-Ar age of 11.2 ± 1.3 Ma from the rhyodacite flow (Tcsf) is erroneous, inconsistent with its stratigraphic position, and that the younger K-Ar ages of 4.16 ± 1.81 Ma and 3.7 ± 0.9 Ma, previously interpreted to crosscut this flow, were actually collected from the primary lava flow and its coeval feeder dike, respectively.

We revisited this capping rhyodacite flow and nearby dikes to assess their relative age and emplacement mechanisms. The 3.7 ± 0.9 Ma dike outcrop on the eastern bank of arroyo 1 (Tcsd) is at least 5 m wide and exhibits a strong northeast-southwest–striking vertical foliation (Fig. 2). The same dike is exposed along strike to the southwest, across arroyo 1, and continues up the eastern flank of Hast Pitzcal. Here the dike thickens to 20–40 m wide, crosscuts marine and nonmarine conglomerate beds, and crops out continuously up to the base of the rhyodacite flow (Figs. 2, 13F, and 14A; 500–600 m on horizontal distance scale). The dike does not cut through the rhyodacite flow. Instead, we observe the subhorizontal rhyodacite flow as continuous and intact across this dike. In some exposures the dike exhibits continuous foliation with the overlying flow. Gastil et al. (1999) interpreted the flow as an ash-flow tuff that consists of a basal pumice bed, overlain by a breccia flow, overlain by a vitrophyric welded tuff, overlain by a crystal-rich effusive rhyolite. Our observations confirm that the base of the flow is underlain by thin and discontinuous deposits of pyroclastic material (unit Tcsp).The majority of the Rhyodacite of Cerro Starship consists of a lava flow. This is supported by the observation that both the matrix of the basal vitrophyre and that of the main flow deposit do not consist of ash or other pyroclastic material (e.g., pumice, lithic fragments), and instead exhibit irregular flow foliation (Figs. 2, 13E, and 14A) typical of felsic lava flows (Cas and Wright, 1987).

We also revisited the southern end of the main, elongate flow body (Fig. 2) where Gastil et al. (1999) interpreted the 4.16 ± 1.81 Ma (K-Ar) age from it to be from a crosscutting dike. We do not observe dikes exposed along the continuous, undulatory upper flow surface (Fig. 13C) or where the subhorizontal, basal contact of the flow is well exposed in a vertical cliff exposure (Fig. 13H). In summary, our observations concur with the interpretation in Oskin and Stock (2003a) that the dike (Tcsd) fed the capping rhyodacite flow (Tcsf). The main fissure-fed rhyodacite flow deposit was likely sourced from an ~600-m-long portion of the dike that is continuous with the dike exposure on the northeastern flank of Hast Pitzcal, but is currently unexposed, beneath Hast Pitzcal. As additional support of this hypothesis, we find that basal pyroclastic deposits (Tcsp) are limited to an area immediately south of the point where this dike intersects the flow (Fig. 2).

To resolve disparate interpretations of the age of the rhyodacite, we dated a sample from basal Tcsf, away from any mapped dikes, where its sharp subhorizontal basal contact is well exposed (Fig. 2). Our ages of 3.51 ± 0.05 Ma (Ar/Ar) and 4.13 ± 0.09 Ma (U/Pb) are consistent with previously published K-Ar ages of 3.7 ± 0.9 Ma on the arroyo 1 feeder dike (Gastil and Krummenacher, 1977b) and 4.16 ± 1.81 Ma from the top of the flow (Neuhaus, 1989).

Altogether, these data confirm that the K-Ar age of 11.2 ± 1.3 Ma by Gastil and Krummenacher (1977b) does not represent the age of the flow and should not be used as a minimum age constraint on marine sedimentation on SWIT.

REGIONAL IMPLICATIONS

A latest Miocene to Pliocene interpretation for the age of the SWIT marine basin has important regional implications for the tectonic evolution of the Gulf of California rift and marine incursion into it. Below, we discuss these implications and develop a paleogeographic reconstruction of a narrow marine embayment that formed during the earliest stages of oblique opening of the northern Gulf of California rift. This integrated analysis illustrates the relationship between marine basin formation and the geodynamic evolution of this portion of the Pacific–North America plate boundary.

Synchronous Marine Incursion into the Northern Proto–Gulf of California

A revised latest Miocene age for the earliest marine deposits on Isla Tiburón is consistent with a regionally synchronous marine incursion, no earlier than 6.5 Ma, into basins of the northern Gulf of California and basins now buried by continental deposits in the Salton Trough (southern California) and Altar basin (northwestern Sonora, México). Throughout this region (Fig. 16A) all timing information for marine incursion established through clear crosscutting relationships and/or confidently in situ microfossil assemblages indicates that marine conditions first existed here between 6.5 and 6.0 Ma (e.g., Martín-Barajas et al., 1997, 2001; Stock, 1997; McDougall et al., 1999; Oskin and Stock, 2003a; McDougall, 2008; Dorsey et al., 2011; this study). This late Miocene marine incursion (Fig. 16B) likely occurred along a relatively narrow and incipient set of en echelon pull-apart basins formed within an ~600-km-long portion of the Gulf of California shear zone (Bennett and Oskin, 2014), a transtensional portion of the Pacific–North America plate boundary. Marine incursion into the northern Gulf of California and Salton Trough appears to have shortly followed the ca. 7 Ma marine incursion documented in the central Gulf of California (Holt et al., 2000; Conly et al., 2005; Miranda-Avilés et al., 2005; Miller and Lizarralde, 2013).

The question of whether latest Miocene marine incursion was preceded by an earlier, middle Miocene marine seaway remains controversial. Middle Miocene microfossils are reported from the northern Salton Trough (McDougall et al., 1999), Cerro Prieto (Cotton and Vonder Haar, 1980), Laguna Salada (Martín-Barajas et al., 2001), near San Felipe (Boehm, 1984), from wells in the northern Gulf of California and southern Salton Trough (Helenes et al., 2009), in the coastal Sonora plains southeast of Bahía de Kino (Gómez-Ponce, 1971), and on Tres Marías Islands at the mouth of the Gulf of California (Figs. 1A and 16A; Carreño, 1985) (see regional summary in Carreño and Smith, 2007). At most of these localities, the middle Miocene microfossils were considered to be reworked and not in situ specimens. For example, both middle Miocene and Cretaceous microfossils were observed in Cerro Prieto geothermal wells (Cotton and Vonder Haar, 1980), suggesting that the deposits hosting these specimens likely postdate arrival of the Colorado River, which is dated as 5.3 Ma (Dorsey et al., 2007, 2011). In one possible exception, lower Miocene specimens have been documented from depths of ~250–750 m in water wells in coastal southern Sonora (Fig. 16A; Gómez-Ponce, 1971). However, Winker (1987) discounted the in situ status of these specimens due to the unavailability of samples and necessary documentation. In addition, Gastil and Krummenacher (1977b, p.194) reported an oral communication with James Ingle, who believed that the identification of lower Miocene microfossils in the coastal Sonora water wells was not reliable, and the strata could postdate 10 Ma. No such marine rocks occur in mountain ranges that flank the modern-day Sonora coastline, despite evidence for significant faulting, tilting, and basin formation ca. 9–6 Ma (Herman and Gans, 2006; Seiler et al., 2010; Darin, 2011; Bennett et al., 2013).

A second, more widely cited report of in situ middle Miocene microfossils is based on analysis of cuttings from four Petróleos Mexicanos (PEMEX, 1985) exploration wells in the northern Gulf of California (Helenes et al., 2009) (Fig. 16A). Helenes et al. (2009) reported in situ dinoflagellates and calcareous nannofossils that suggest the presence of as much as 3750 m of early to middle Miocene (pre–11.6 Ma) marine deposits in the Wagner and Consag pull-apart basins, in the western part of the northern Gulf of California. This contradicts other published studies that found that transtensional marine basins in the western Gulf rift began opening ca. 3.3–2.0 Ma, not in middle Miocene time (Nagy and Stock, 2000; Stock, 2000; Aragón-Arreola and Martín-Barajas, 2007). Helenes et al. (2009) concluded that the lower 1833 m of marine deposits in the upper Tiburón basin, offshore SWIT (Fig. 16), are middle Miocene age, and geophysical evidence indicates the presence of ~1000 m of additional sediments below the bottom of the well. This lower interval correlates to sedimentary unit A of Aragón-Arreola and Martín-Barajas (2007), and would require that a marine seaway, at least 50 km wide, existed between the now-submerged continental shelves of Isla Tiburón, Sonora, and northeastern Baja California prior to 11.6 Ma. This interpretation is at odds with onshore evidence that significant rift-related faulting in the region did not begin until after 12.5–11 Ma (Stock and Hodges, 1990; Lee et al., 1996; Lewis and Stock, 1998). The existence of a middle Miocene marine basin of this extent also contradicts onshore timing constraints for the opening of the northern Gulf of California, that restore the modern shorelines and outcrops of several extensive late Miocene ash-flow tuffs to close proximity ca. 6 Ma (Fig. 16B; Oskin et al., 2001; Oskin and Stock, 2003b). It is important that no major intervals of ash deposits are described from the upper Tiburón PEMEX well, despite the presence of several hundred meters of these late Miocene tuffs on the basin margins.

Helenes et al. (2009) questioned the validity of the cross-gulf tie point (tuffs) in Oskin et al. (2001) and Oskin and Stock (2003b), suggesting that the correlation of these once-proximal volcanic deposits may be erroneous because paleomagnetic results would not detect longitudinal (east-west) motion of Baja

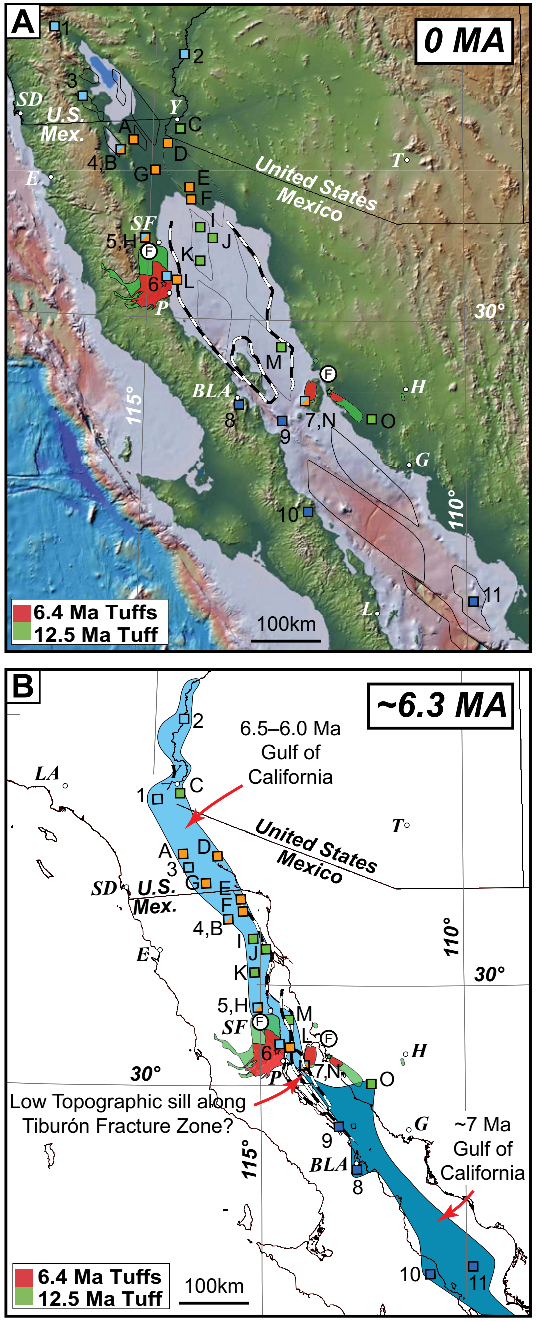

- middle Miocene microfossils, considered *in situ* by original author(s) of cited paper
- middle Miocene microfossils, reworked
- earliest marine deposits of central Gulf of California, ca. 7 Ma
- earliest marine deposits of northern Gulf of California and Salton Trough, ca. 6.5–6.0 Ma
- earliest marine deposits ca. 6.5–6.0 Ma containing reworked middle Miocene microfossils
- Ⓕ correlative fusilinid-rich clast conglomerate (Gastil et al., 1973)
- approximate ignimbrite vent location
- ○ city
- approximate edge of thick continental crust (after Aragón-Arreola and Martín-Barajas, 2007; Mar-Hernández et al., 2012)
- rift-related pull-apart basins (after Aragón-Arreola and Martín-Barajas, 2007; Miller and Lizarralde, 2013)

Earliest Marine Deposits

(1) Imperial Fm, San Gorgonio Pass [6.5–6.3 Ma], McDougall et al. (1999)
(2) Bouse Fm, Blythe basin [8.1–5.3 Ma], McDougall and Miranda-Martínez (2014)
Note for pt #2: The Bouse Fm is likely younger than 6.0 Ma (House et al., 2008) and may be 5.6–5.3 Ma (McDougall and Miranda-Martínez, 2014), and if so, this location of marine deposits would post-date our ~6.3 Ma reconstruction in panel B.
(3) Fish Creek Gypsum, Split Mtn. Gorge [6.3 Ma], Dean (1996); Dorsey et al. (2007, 2011)
(4) Cerro Colorado basin (Laguna Salada) [8–6 Ma], Martin-Barajas et al. (2001)
(5) San Felipe Marine Sequence [6.0 Ma], Boehm (1984); Stock (1997)
(6) Puertecitos Fm [<6.1 Ma], Martin-Barajas et al. (1997)
(7) Southwest Isla Tiburon [6.4–6.0 Ma], Gastil et al. (1999); Oskin & Stock (2003a); This Study
(8) Bahia de los Angeles [<12.1 Ma], Delgado-Argote et al. (2000)
(9) San Lorenzo Archipelago [7.8–5.0 Ma], Escalona-Alcázar et al. (2001)
(10) Boleo Fm, Santa Rosalia [~7 Ma], Holt et al. (2000); Miranda-Avilés et al. (2005)
(11) Marine Evaporite, East Guaymas embayment [~7 Ma], Miller and Lizarralde (2013)

Middle Miocene Microfossils

(A) Cerro Prieto geothermal wells, Cotton & Vonder Haar (1980)
(B) Cerro Colorado basin (Laguna Salada), Martin-Barajas et al. (2001)
(C) Yuma wells, McDougall (2008)
(D) Well A-1 (Altar basin), Helenes et al. (2009)
(E) Well A-2, Altar basin), Helenes et al. (2009)
(F) Well A-3 (Altar basin), Helenes et al. (2009)
(G) Well D (Colorado River delta), Helenes et al. (2009)
(H) San Felipe marine sequence, Boehm (1984)
(I) Well W-1 (Wagner basin), Helenes et al. (2009)
(J) Well W-2 (Wagner basin), Helenes et al. (2009)
(K) Well C (Consag basin), Helenes et al. (2009)
(L) Well P (Puertecitos shelf), Helenes et al. (2009)
(M) Well T (Tiburon basin), Helenes et al. (2009)
(N) Southwest Isla Tiburon basin, Gastil et al. (1999)
(O) Water wells (coastal Sonora plain), Gomez-Ponce (1971)

Figure 16. (A) Modern-day location of key marine strata and fossil localities showing exposures of late Miocene (6.5–6.0) marine rocks with isotopic age constraints in the northern Gulf of California and Salton Trough (light blue squares), and slightly older, late Miocene (ca. 7 Ma) marine rocks, or poorly constrained localities (locale 8) of the central Gulf of California (dark blue squares). Basins or wells containing middle Miocene microfossils that are either reworked (orange squares) or considered in situ by the original authors (green squares) are shown. Pull-apart basins (thin black lines) are after Aragón-Arreola and Martín-Barajas (2007) and Miller and Lizarralde (2013). Physiographic base map is from GeoMapApp (www.geomapapp.org). Cities abbreviated in italics: LA—Los Angeles, SD—San Diego, E—Ensenada, Y—Yuma, T—Tucson, SF—San Felipe, P—Puertecitos, BLA—Bahía de Los Angeles, H—Hermosillo, G—Guaymas, L—Loreto. (B) Earliest Gulf of California seaway (blue) during late Miocene time (ca. 6.3 Ma). Same features as in A are restored to their ca. 6.3 Ma position. This reconstruction restores the Baja California peninsula 235 km to the southeast, matching correlative outcrops of the 12.5 Ma tuff of San Felipe and the 6.4 Ma tuffs of Mesa Cuadrada (Oskin et al., 2001; Oskin and Stock 2003b), while honoring minimal overlap of the relatively thick continental crust and shallow basement geophysically imaged offshore Isla Tiburón and northeastern Baja California (Aragón-Arreola and Martín-Barajas, 2007; Mar-Hernández et al., 2012). Tens of kilometers of dextral deformation in northeastern Baja California (Lewis and Stock, 1998) and tens of kilometers of pre–6 Ma dextral faulting in coastal Sonora (Bennett et al., 2013) are not accounted for in this reconstruction. These onshore displacements play little to no role in the ca. 6.3 Ma position of the offshore and coastal features restored in this reconstruction.

California during subsequent rifting. Helenes et al. (2009) may have misconstrued the paleomagnetic data presented in Oskin et al. (2001) as a direct measure of paleolatitude through its relationship to paleomagnetic inclination (e.g., Butler, 1992). Correlation of these tuffs across the Gulf of California is based on their unique paleomagnetic remanence vector directions (Lewis and Stock, 1998; Stock et al., 1999; Bennett and Oskin, 2014), tuff lithologies, cooling-unit stratigraphy, whole-rock and phenocryst geochemistry (Oskin and Stock, 2003b), and geochronologic ages (Bennett et al., 2013). Their original proximity was not based on paleolatitude interpretations from paleomagnetic data, but rather the thickness and outcrop distribution of multiple tuff markers and correlation of internal cooling units (Oskin and Stock, 2003b). This cross-gulf tuff correlation is robust and must be considered in any discussion regarding the tectonic evolution of, or marine seaway incursion into, the northern Gulf of California.

A middle Miocene interpretation for basal sediments in the offshore PEMEX wells is also at odds with abundant evidence for a late Miocene to Pliocene age of earliest marine deposits in numerous locations around the northern Gulf of California (e.g., Escalona-Alcázar et al., 2001) and Salton Trough region (e.g., McDougall et al., 1999; Pacheco et al., 2006; Dorsey et al., 2007, 2011). A geochemical provenance study found that fine-grained marine deposits in deep PEMEX wells in the northern Gulf of California are mostly derived from the Colorado River watershed (Lomtatidze-Jiménez, 2013), and thus must postdate the 5.3 Ma first arrival of the Colorado River in the Gulf of California–Salton Trough basin (Dorsey et al., 2007, 2011).

To reconcile the paleontological results with onshore geologic constraints, we suggest that the specimens asserted to be in situ by Helenes et al. (2009) likely are instead reworked specimens. Reworked microfossils are observed at a higher interval in the upper Tiburón well, and a late Miocene calcareous nannofossil (*Sphenolithus neoabies*) is reported at a depth of 3470 m in deposits interpreted by Helenes et al. (2009) to be early to middle Miocene in age. Age determinations of sediments bearing fossils of mixed ages must always be based on the youngest fossils present, because of the possibility that the sediments contain older reworked fossils. PEMEX (1985) considered *S. neoabies* to be latest Miocene to Pliocene in age (6–3 Ma). Application of this age to basal marine deposits (unit A) that also contain this species in the Altar basin (Pacheco et al., 2006) would permit correlation to the lower interval in the upper Tiburón basin. Moreover, unit A where documented by Pacheco et al. (2006) in the Altar basin contains clinoforms of Colorado River delta sands, and thus must postdate the ca 5.3 Ma arrival of the Colorado River into the northernmost Gulf of California (Dorsey et al., 2007, 2011). Although the first appearance of *S. neoabies* may be middle Miocene (ca. 11.8 Ma) (Perch-Nielsen, 1985), the lower part of its range is speculative (McDougall, 2008).

Honoring age constraints from correlative tuffs (Oskin et al., 2001; Oskin and Stock, 2003b) and geophysical data for the extent of continental crust submerged beneath the northern Gulf of California (Aragón-Arreola and Martín-Barajas, 2007; Mar-Hernández et al., 2012; Martín-Barajas et al., 2013), we present a revised reconstruction of the northern Gulf of California at latest Miocene time with the reconstructed locations of observed Miocene marine strata (Fig. 16B). In order to avoid substantial overlap of relatively thick continental crust (i.e., shallow depth to basement) identified by Martín-Barajas et al. (2013), this reconstruction restores Baja California 235 km to the southeast, 10 km less than the minimum distance estimated in Oskin and Stock (2003b) (255 ± 10 km). This reconstruction aligns the western edge of an ~25-km-wide submerged continental shelf offshore western Isla Tiburón with the eastern edge of an ~10–15-km-wide shelf offshore Puertecitos, Baja California (distances measured northwest-southeast, parallel to relative plate motion). Thus, in latest Miocene time during marine deposition on SWIT, the maximum possible distance between the Isla Tiburón and Baja California coastlines was ~35–40 km (Fig. 16B), leaving little space for an extensive middle Miocene marine basin. In addition, an exploration well drilled on the outboard edge of the Puertecitos shelf (location L in Fig. 16) encountered only late Miocene strata that overlie an 8 ± 1 Ma andesite directly overlying crystalline basement (PEMEX, 1985), further limiting the extent of a seaway here. We therefore conclude that the more extensive deposits of unit A in the upper Tiburón basin (line 2D of Aragón-Arreola and Martín-Barajas, 2007), that correlate to the middle Miocene interval of Helenes et al. (2009), are unlikely to be middle Miocene age. Instead, these lowermost upper Tiburón basin marine deposits probably began to accumulate during late Miocene time (ca. 6.5–6.0 Ma), coincident with deposition of marine deposits on SWIT, when the upper Tiburón basin began to rapidly widen and subside due to localized oblique divergence along the Pacific–North America plate boundary (Oskin et al., 2001).

Possible Origins of Reworked Middle Miocene Microfossils

Although we contend that in situ middle Miocene microfossils have not been convincingly documented from marine deposits in or adjacent to the Gulf of California, the presence of reworked middle Miocene marine microfossils in the Gulf of California and Salton Trough (McDougall, 2008) suggests that marine conditions existed somewhere in the region during middle Miocene time. Here we explore three potential origins of these reworked microfossils, and suggest that they may have been eroded from middle Miocene strata either within or beyond the Gulf of California rift.

One possible source for middle Miocene reworked microfossils is a middle Miocene seaway that was broadly coincident with the late Miocene Gulf of California rift axis, as proposed by Helenes and Carreño (1999). Such a seaway likely would have been considerably smaller and more discontinuous than the well-documented late Miocene seaway (blue squares in Fig. 16B). A marine basin in this location could have connected to the Pacific Ocean via a seaway that transected the Baja California peninsula (e.g., Helenes and Carreño, 1999; Dolby et al., in press). However, upon restoration of the Baja California peninsula (e.g., Fig. 16B) any potential middle Miocene transpeninsular seaway is located hundreds of kilometers southeast of the paleontological evidence for such a seaway. A southern connection to the Pacific is even farther, and also unlikely because marine deposition in the southern Gulf of California occurred later, ca. 10–7 Ma (see summary by Oskin and Stock, 2003a). A northern connection to the Pacific Ocean is also doubtful due to dissimilar middle Miocene microfossil assemblages documented in the Los Angeles Basin (temperate) and the Salton Trough and northern Gulf of California (tropical) (Helenes and Carreño 1999). If a middle Miocene basin or embayment existed, portions of it that contained middle Miocene microfossils could have been exposed and eroded during subsequent rift-related faulting, contributing specimens to the late Miocene basins. However, geologic constraints that tie the margins of the Gulf of California into close proximity at late Miocene time (Oskin et al., 2001) make it difficult to argue for a middle Miocene seaway in the current location of the Gulf of California.

Another possible source may have been a shallow seaway that may have existed in an area of middle Miocene backarc extension located northeast of and parallel to the present-day Gulf of California, in Sonora and Sinaloa (Fig. 17). Such a middle Miocene backarc basin would have existed northeast of a northwest-southeast chain of middle Miocene volcanic centers, in the wake of the southwestward-migrating volcanic arc (Karig and Jensky, 1972; Hausback, 1984; Dorsey and Burns, 1994; Ferrari et al., 1999; Umhoefer et al., 2001), as proposed in previous studies (Fenby and Gastil, 1991; Smith, 1991; Helenes and Carreño, 1999). A marine backarc basin in this location would require similar connections to the Pacific Ocean, as discussed herein. Subsequent uplift and exposure of these marine deposits could have eroded and transported middle Miocene microfossils into the latest Miocene marine basins in the northern Gulf of California via roughly southwest-directed drainages (Fig. 17). It is important that no outcrops of middle Miocene marine strata are known anywhere in western Mexico, despite the documented presence of nonmarine strata of the appropriate age (Herman and Gans, 2006; Darin, 2011; Bennett et al., 2013). This does not support the concept of a middle Miocene seaway, whether located beneath the modern-day Gulf of California or in a middle Miocene backarc basin. Regionally extensive outcrops of the 12.5 Ma tuff of San Felipe (Fig. 16; Stock et al., 2006; Bennett and Oskin, 2014) do not overlie marine sedimentary rocks, as would be expected if extensive marine basins existed during middle Miocene time. If microfossils recorded from beneath the coastal Sonora plain (Gómez-Ponce, 1971) are in situ specimens, and if subsurface deposits beneath Yuma, Arizona (McDougall, 2008) are middle Miocene age, these two localities (Fig. 16) may be the only subsurface remnants of this hypothetical middle Miocene backarc basin seaway, distinct from the late Miocene to present Gulf of California in both time and space.

A third possible source for reworked middle Miocene microfossils is the continental shelf on the Pacific side of the southernmost Baja California peninsula, adjacent to the mouth of the Gulf of California (Fig. 17). Middle Miocene marine strata in this area were exposed to wave-base erosion after deposition (Brothers et al., 2012) and could have contributed middle Miocene marine microfossils to late Miocene basins 700–900 km away, as marine waters progressively spilled northwestward into intrarift transtensional basins of the proto–Gulf of California. Mobilization, long-distance transport, and redeposition of microfossils are documented elsewhere, supporting interpretations for 800 to >2000 km transport by wind (Goudie and Sperling, 1977), pyroclastic volcanic eruptions (Van Eaton et al., 2013), and suspended load currents (Otvos and Bock, 1976). Further work is required to support this long-distance source, such as documentation of microfossils species at this possible source location. Additional documentation of reworked middle Miocene microfossils in late Miocene marine sections throughout the Gulf of California is also necessary, similar to reports of reworked middle Miocene microfossils on Tres Marías Islands (Carreño, 1985; McCloy et al., 1988), in the Laguna Salada basin (Martín-Barajas et al., 2001), and in late Miocene deposits within the upper Tiburón basin (Helenes et al., 2009).

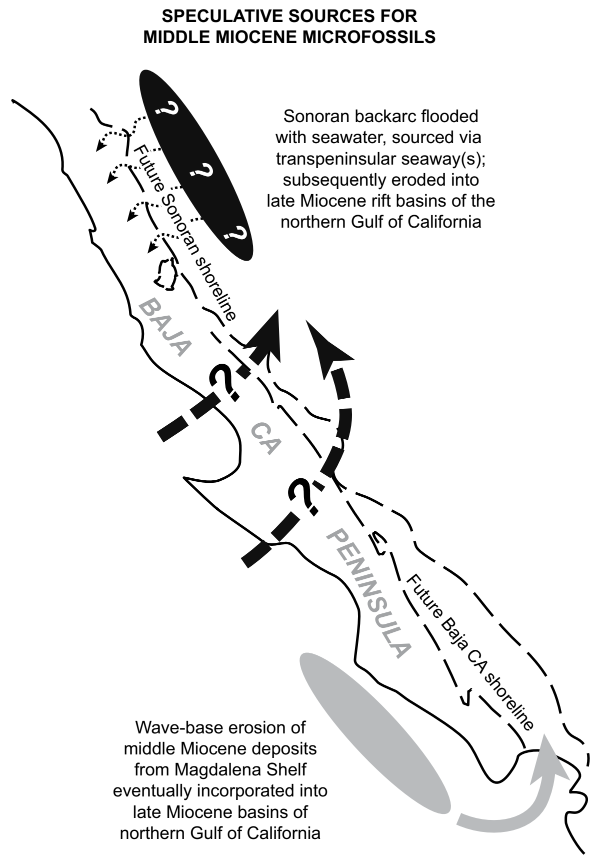

Figure 17. Schematic map of northwestern Mexico during middle Miocene time, prior to opening of the Gulf of California (CA—California). Speculative sources of middle Miocene marine microfossils include a flooded backarc basin in modern-day western Sonora or marine deposits from the southern Baja California shelf. See text for details.

Tectonic Evolution of the Gulf of California

Synchronous late Miocene marine incursion along the Pacific–North America plate boundary is a critical event in the tectonic and paleogeographic evolution of the Gulf of California rift. A major geodynamic change must have occurred for this region to evolve from a subaerial volcanic arc at the end of middle Miocene time (Hausback, 1984; Dorsey and Burns, 1994; Umhoefer et al., 2001) to a system of submarine pull-apart basins by the end of Miocene time. Such a substantial modification of regional topography implies significant crustal thinning and related subsidence. The late Miocene marine incursion was spatially coincident with, and occurred soon after the development of, the Gulf of California shear zone, an ~50–100-km-wide belt of localized strike-slip faulting and related clockwise vertical-axis block rotations, crustal thinning, and regional subsidence (Fig. 16B; Bennett and Oskin, 2014). The Gulf of California shear zone created a series of fault-bounded nonmarine transtensional basins ca. 9–6 Ma (Bennett and Oskin, 2014), now preserved on the conjugate rift margins in eastern Baja California and coastal Sonora (Seiler et al., 2010; Bennett et al., 2013). South of Isla Tiburón, marine incursion reached the Guaymas basin in the central Gulf of California ca. 7 Ma (Holt et al., 2000; Conly et al., 2005; Miranda-Avilés et al., 2005; Miller and Lizarralde, 2013), coincident with this transtensional deformation (Miller and Lizarralde, 2013).

Studies from San Gorgonio Pass in the north (McDougall et al., 1999; McDougall, 2008) to Isla Tiburón in the south (Gastil et al., 1999; this study) support the widespread onset of earliest marine conditions in the northern Gulf of California and Salton Trough ca. 6.5–6.0 Ma, following this onset of significant transtensional relative plate motion across the northern Gulf of California. Flooding of marine waters into the northern Gulf of California may have been delayed by as much as 1 m.y. by a topographic barrier formed by the Tiburón transform fault, which separated areas of oblique crustal thinning and subsidence in the upper Tiburón basin to the northwest from the lower Tiburón and Guaymas basins to the southeast. As the Baja California peninsula was translated to the northwest along the Tiburón transform fault, a low topographic spill point may have formed between these areas, allowing seawater to enter the sub-sea-level basins of the northern Gulf of California and Salton Trough (Fig. 16B), similar to earlier spillover events envisioned in the eastern Guaymas Basin to the south (Miller and Lizarralde, 2013). Once the topographic barrier between the lower Tiburón basin and Guaymas Basin was breached, a spillover event probably resulted in very rapid marine flooding of basins for hundreds of kilometers along the plate boundary into the northern Gulf of California and Salton Trough (e.g., Umhoefer et al., 2013). Thus the formation of a proto–Gulf of California seaway likely was intimately linked, in time and space, to the onset of focused oblique rifting, which became localized in the northern Gulf of California region near the end of Miocene time (Oskin et al., 2001; Bennett et al., 2013). Post–6 Ma Pacific–North America relative plate motion subsequently localized into the core of the Gulf of California shear zone, rifted apart these regions of nonmarine transtensional basins, and widened the Gulf of California seaway (e.g., Oskin and Stock, 2003b).

CONCLUSIONS

Isotopic and biostratigraphic data conclusively show that marine strata on SWIT range in age from late Miocene to early Pliocene. The timing of earliest marine deposition is constrained by the 6.44 ± 0.05 Ma tuff of Hast Pitzcal that underlies the oldest marine deposits, and the 6.01 ± 0.20 Ma tuff of Oyster Amphitheater that is interbedded near the base of the marine section. Marine sedimentation in the study area ceased prior to subaerial eruption of the 3.51 ± 0.05 Ma to 4.13 ± 0.09 Ma rhyodacite of Cerro Starship and the 4.34 ± 0.20 Ma tuffs of Hipat Mesa. These age constraints are consistent with the microfossil assemblage from the same section that independently yielded an age of 6.2–4.3 Ma for marine deposits of SWIT (Gastil et al., 1999). A revised depositional environment interpretation, that much of the SWIT marine deposits are inclined foreset deposits in a prograding Gilbert-type fan delta system, supports a total maximum basin thickness of ~300 m, rather than the >1500 m basin thickness suggested by previous studies that interpreted these inclined deposits as thick basin strata that were subsequently tectonically tilted.

New detailed geologic mapping and modern geochronologic data demonstrate that previous interpretations for the age and depositional environment of marine deposits on SWIT were based on incorrect K-Ar results and misinterpretation of field relationships, in part due to the structural complexity of the area. The previously proposed upper age constraint of 11.2 ± 1.3 Ma from the capping Rhyodacite of Cerro Starship (Gastil and Krummenacher, 1977b) is an erroneous age that is inconsistent with all other, newer age dates and well-established crosscutting relationships. The 12.9 ± 0.4 Ma age reported by Smith et al. (1985) (redated here to 18.70 ± 0.19 Ma) is from a volcanic unit underlying, rather than interstratified with, the marine deposits. Our results are at odds with a study that proposed widespread middle Miocene deposits in offshore marine basins (Helenes et al., 2009), and refute the use of the SWIT marine deposits as a reference section for middle Miocene macrofauna (Smith, 1991). A late Miocene age for the SWIT marine basin is consistent with regional marine incursion into the northern proto–Gulf of California no earlier than 6.5 Ma (Oskin and Stock, 2003a). Regional marine incursion occurred along a narrow, >500-km-long fault-bounded seaway, from at least Isla Tiburón in the south to San Gorgonio Pass in the north, between 6.5 and 6.0 Ma.

Middle Miocene microfossils documented at some locations in the Gulf of California and Salton Trough region are unlikely to be in situ. Rather, these specimens probably are reworked into late Miocene strata from older deposits, as documented in several onshore exposures (e.g., McDougall, 2008). The locations of sources for middle Miocene microfossils remain unclear and the subject of ongoing speculation. We suggest that the most likely sources for reworked middle Miocene microfossils are (1) a marine extensional backarc basin in the northwestern Mexican Basin and Range province for which outcrops are not known, or (2) middle Miocene marine deposits along the western continental shelf of southernmost Baja California that were exposed to wave-base erosion during late Miocene time (Brothers et al., 2012).

Late Miocene marine incursion into the northern Gulf of California resulted from focused oblique extension, crustal thinning, and resulting tectonic subsidence. This narrow, late Miocene seaway was colocated with, and flooded immediately following the development of, the Gulf of California shear zone, a narrow belt of localized strike-slip faulting, clockwise block rotation, and formation of pull-apart basins (Bennett and Oskin, 2014). Resolution of the controversy over the age of oldest marine deposits on SWIT provides a critical step forward in a long-standing debate over the age of marine sedimentation in the northern Gulf of California. Improved age constraints on marine deposition provide important new insights into late Miocene focused deformation related to localization of the Pacific–North America transtensional plate boundary in the northern Gulf of California and Salton Trough region.

ACKNOWLEDGMENTS

Funding from the National Science Foundation (grants EAR-0739017 and EAR-0904337 to Oskin, EAR-0738723 and EAR-0948170 to Dorsey) made this research possible. Permission to enter Isla Tiburón was granted by the Secretaría de Medio Ambiente y Recursos Naturales–Comisión Nacional de Areas Naturales Protegidas and the native Cumcaác (Seri) tribe. We thank Arturo Martín-Barajas for assistance with permit acquisition. This study benefited from insightful discussions with Judith Smith, Kristin McDougall, Arturo Martín-Barajas, Adam Forte, and Austin Elliott. A U.S. Geological Survey review by Robert Powell and *Geosphere* reviews by Joann Stock, Paul Umhoefer, and Associate Editor Derek Keir helped improve the manuscript. Micahel Tappa, Jordan Ford, Nicholas Buckmaster, and Molly Keogh all provided great company, safety, and assistance while conducting field work on Isla Tiburón. Tom Donovan, Gregory Smart, and the Prescott College Kino Bay Center for Cultural and Ecological Studies staff provided incredible logistical support and comfortable accommodations while conducting field work. We thank Ernesto Molina Villa-Lobos of the native Cumcaác (Seri) tribe for his superb boatmanship and safekeeping during our field research. Any use of trade, product, or firm names is for descriptive purposes only and does not imply endorsement by the U.S. Government.

REFERENCES CITED

Abbott, P.L., and Smith, T.E., 1989, Sonora, Mexico, source for the Eocene Poway Conglomerate of southern California: Geology, v. 17, p. 329–332, doi:10.1130/0091-7613(1989)017<0329:SMSFTE>2.3.CO;2.

Andersen, T., 2002, Correction of common lead in U-Pb analyses that do not report Pb-204: Chemical Geology, v. 192, no. 1-2, p. 59–79.

Aragón-Arreola, M., and Martín-Barajas, A., 2007, Westward migration of extension in the northern Gulf of California, Mexico: Geology, v. 35, p. 571–574, doi:10.1130/G23360A.1.

Bennett, S.E.K., 2013, The role of rift obliquity in formation of the Gulf of California [Ph.D. thesis]: Davis, University of California–Davis, 220 p.

Bennett, S.E.K., and Oskin, M.E., 2014, Oblique rifting ruptures continents: Example from the Gulf of California shear zone: Geology, v. 42, p. 215–218, doi:10.1130/G34904.1.

Bennett, S.E.K., Oskin, M.E., and Iriondo, A., 2013, Transtensional rifting in the proto-Gulf of California, near Bahía Kino, Sonora, México: Geological Society of America Bulletin, v. 125, p. 1752–1782, doi:10.1130/B30676.1.

Boehm, M.C., 1984, An overview of the lithostratigraphy, biostratigraphy, and paleoenvironments of the late Neogene San Felipe Marine Sequence, Baja California, Mexico, *in* Frizzell, V.A., ed., Geology of the Baja California Peninsula: Pacific Section, Society of Economic Paleontologists and Mineralogists Book 39, p. 253–265.

Brothers, D., Harding, A., Gonzalez-Fernandez, A., Holbrook, W.S., Kent, G., Driscoll, N., Fletcher, J., Lizarralde, D., Umhoefer, P., and Axen, G., 2012, Farallon slab detachment and deformation of the Magdalena Shelf, southern Baja California: Geophysical Research Letters, v. 39, L09307, doi:10.1029/2011GL050828.

Butler, R.L., 1992, Paleomagnetism: Cambridge, Massachusetts, Blackwell Scientific Publications, 319 p.

Carreño, A. L., 1985, Biostratigraphy of the Late Miocene to Pliocene on the Pacific island Maria Madre, Mexico: Micropaleontology, v. 31, p. 139–166, doi:10.2307/1485482.

Carreño, A.L., 1992, Neogene microfossils from the Santiago Diatomite, Baja California Sur, Mexico: Paleontología Mexicana, v. 59, p. 1–37.

Carreño, A.L., and Smith, J.T., 2007, Stratigraphy and correlation for the ancient Gulf of California and Baja California peninsula, Mexico: Bulletins of American Paleontology, v. 371, 146 p.

Cas, R.A.F., and Wright, J.V., 1987, Volcanic successions, modern and ancient, London, Allen and Unwin, 528 p.

Cassidy, M., 1990, Marine stratigraphy and paleontology of southwest Isla Tiburón, Gulf of California, Mexico [M.S. thesis]: San Diego, California, San Diego State University, 177 p.

Conly, A.G., Brenan, J.M., Bellon, H., and Scott, S.D., 2005, Arc to rift transitional volcanism in the Santa Rosalía region, Baja California Sur, Mexico: Journal of Volcanology and Geothermal Research, v. 142, p. 303–341, doi:10.1016/j.jvolgeores.2004.11.013.

Cotton, M.L., and Vonder Haar, S., 1980, Microfossils from Cerro Prieto geothermal wells, Baja California, Mexico, *in* Conference proceedings: 2. Symposium on the Cerro Prieto Geothermal Field, Baja California, Mexico: http://www.osti.gov/scitech/servlets/purl/5384920, 11 p.

Darin, M.H., 2011, Late Miocene extensional deformation in the Sierra Bacha, coastal Sonora, México: Implications for the kinematic evolution of the proto-Gulf of California [M.S. thesis]: Eugene, University of Oregon, 95 p.

Dean, M.A., 1996, Neogene Fish Creek Gypsum and associated stratigraphy and paleontology, southwestern Salton Trough, California, *in* Abbott, P.L., and Seymour, D.C., eds., Sturzstroms and detachment faults, Anza-Borrego Desert State Park, California: San Diego, California, South Coast Geological Society Annual Field Trip Guidebook 24, p. 123–148.

Delgado-Argote, L.A., López-Martínez, M., and Perrilliat, M.C., 2000, Geologic reconnaissance and Miocene age of volcanism and associated fauna from sediments of Bahia de Los Angeles, Baja California, central Gulf of California, *in* Stock, J., et al., eds., Cenozoic tectonics and volcanism of Mexico: Geological Society of America Special Paper 334, p. 111–121, doi:10.1130/0-8137-2334-5.111.

Dolby, G., Bennett, S.E.K., Lira-Noriega, A., Wilder, B.T., and Munguia-Vega, A., in press, Assessing the geologic and climatic forcing of biodiversity and evolution surrounding the Gulf of California: Journal of the Southwest.

Dorsey, R.J., and Burns, B., 1994, Regional stratigraphy, sedimentology, and tectonic significance of Oligocene–Miocene sedimentary and volcanic rocks, northern Baja California, Mexico: Sedimentary Geology, v. 88, p. 231–251, doi:10.1016/0037-0738(94)90064-7.

Dorsey, R.J., Umhoefer, P.J., and Renne, P.R., 1995, Rapid subsidence and stacked Gilbert-type fan deltas, Pliocene Loreto basin, Baja California Sur, Mexico: Sedimentary Geology, v. 98, p. 181–204, doi:10.1016/0037-0738(95)00032-4.

Dorsey, R.J., Fluette, A., McDougall, K., Housen, B.A., Janecke, S.U., Axen, G.J., and Shirvell, C.R., 2007, Chronology of Miocene–Pliocene deposits at Split Mountain Gorge, southern California: A record of regional tectonics and Colorado River evolution: Geology, v. 35, p. 57–60, doi:10.1130/G23139A.1.

Dorsey, R.J., Housen, B.A., Janecke, S.U., Fanning, C.M., and Spears, A.L.F., 2011, Stratigraphic record of basin development within the San Andreas fault system: Late Cenozoic Fish Creek–Vallecito basin, southern California: Geological Society of America Bulletin, v. 123, p. 771–793, doi:10.1130/B30168.1.

Eberly, L.D., and Stanley, T.B., Jr., 1978, Cenozoic stratigraphy and geologic history of southwestern Arizona: Geological Society of America Bulletin, v. 89, p. 921–940, doi:10.1130/0016-7606(1978)89<921:CSAGHO>2.0.CO;2.

Escalona-Alcázar, F.J., Delgado-Argote, L.A., López-Martínez, M., and Rendón-Márquez, G., 2001, Late Miocene volcanism and marine incursions in the San Lorenzo Archipelago, Gulf of California, Mexico: Revista Mexicana de Ciencias Geológicas, v. 18, p. 111–128.

Falk, P.D., and Dorsey, R.J., 1998, Rapid development of gravely high-density turbidity currents in marine Gilbert-type fan deltas, Loreto Basin, Baja California Sur, Mexico: Sedimentology, v. 45, p. 331–349, doi:10.1046/j.1365-3091.1998.0153e.x.

Farr, T.G., et al., 2007, The shuttle radar topography mission: Reviews of Geophysics, v. 45, RG2004, doi:10.1029/2005RG000183.

Fenby, S.S., and Gastil, R.G., 1991, Geologic-tectonic map of the Gulf of California and surrounding areas, *in* Dauphin, J.P., and Simoneit, B.R.T., eds., The Gulf and Peninsular Province of the Californias: American Association of Petroleum Geologists Memoir 47, p. 79–83, doi:10.1306/M47542C6.

Ferrari, L., Lopez-Martinez, M., Aguirre-Diaz, G., and Carrasco-Nunez, G., 1999, Space-time patterns of Cenozoic arc volcanism in central Mexico: From the Sierra Madre Occidental to the Mexican Volcanic Belt: Geology, v. 27, p. 303–306, doi:10.1130/0091-7613(1999)027<0303:STPOCA>2.3.CO;2.

Fletcher, J.M., Grove, M., Kimbrough, D., Lovera, O., and Gehrels, G.E., 2007, Ridge-trench interactions and the Neogene tectonic evolution of the Magdalena shelf and southern Gulf of California: Insights from detrital zircon U-Pb ages from the Magdalena fan and adjacent areas: Geological Society of America Bulletin, v. 119, p. 1313–1336, doi:10.1130/B26067.1.

Ford, M., Williams, E.A., Malartre, F., and Popescu, S.-M., 2009, Stratigraphic architecture, sedimentology and structure of the Vouraikos Gilbert-type fan delta, Gulf of Corinth, Greece, *in* Nichols, G., et al., eds., Sedimentary processes, environments and basins: A tribute to Peter Friend: Oxford, Blackwell Publishing Ltd., p. 49–90, doi:10.1002/9781444304411.ch4.

Gastil, R.G., and Krummenacher, D., 1977a, Reconnaissance geologic map of coastal Sonora between Puerto Lobos and Bahia Kino: Geological Society of America Map and Chart Series MC-16, scale 1:150,000.

Gastil, R.G., and Krummenacher, D., 1977b, Reconnaissance geology of coastal Sonora between Puerto Lobos and Bahia Kino: Geological Society of America Bulletin, v. 88, p. 189–198, doi:10.1130/0016-7606(1977)88<189:RGOCSB>2.0.CO;2.

Gastil, R.G., and Krummenacher, D., 1978, A reconnaissance geologic map of the west-central part of the state of Nayarit, Mexico: Geological Society of America Map and Chart Series MC-24, scale 1:200,000.

Gastil, R.G., Lemone, D.V., and Stewart, W.J., 1973, Permian fusulinids from near San Felipe, Baja California: American Association of Petroleum Geologists Bulletin, v. 57, p. 746–747.

Gastil, R.G., Krummenacher, D., and Minch, J.A., 1979, The record of Cenozoic volcanism around the Gulf of California: Geological Society of America Bulletin, v. 90, p. 839–857, doi:10.1130/0016-7606(1979)90<839:TROCVA>2.0.CO;2.

Gastil, R.G., Neuhaus, J., Cassidy, M., Smith, J.T., Ingle, J.C., and Krummenacher, D., 1999, Geology and paleontology of southwestern Isla Tiburón, Sonora, Mexico: Revista Mexicana de Ciencias Geológicas, v. 16, no. 1, p. 1–34.

Gawthorpe, R.L., and Colella, A., 1990, Tectonic controls on coarse-grained delta depositional systems in rift basins, *in* Colella, A., and Prior, D.B., eds., Coarse-grained deltas: International Association of Sedimentologists Special Publication 10, p. 113–127, doi:10.1002/9781444303858.ch6.

Gilbert, G.K., 1885, The topographic features of lake shores: U.S. Geological Survey Fifth Annual Report, p. 69–123.

Gómez-Ponce, M., 1971, Sobre la presencia de estratos marinos del Mioceno en el estado de Sonora, Mexico: Revista del Instituto Mexicano del Petroleo, v. 3, no. 4, p. 77–78.

Goudie, A.S., and Sperling, C.H.B., 1977, Long distance transport of foraminiferal tests by wind in the Thar Desert, northwest India: Journal of Sedimentary Petrology, v. 47, p. 630–633, doi:10.1306/212F71FD-2B24-11D7-8648000102C1865D.

Hausback, B.P., 1984, Cenozoic volcanic and tectonic evolution of Baja California Sur, Mexico, *in* Frizzell, V.A., Jr., ed., Geology of the Baja California Peninsula: Pacific Section, Society of Economic Paleontologists and Mineralogists Book 39, p. 219–236.

Helenes, J., and Carreño, A.L., 1999, Neogene sedimentary evolution of Baja California in relation to regional tectonics: Journal of South American Earth Sciences, v. 12, p. 589–605, doi:10.1016/S0895-9811(99)00042-5.

Helenes, J., Carreño, A.L., and Carillo, R.M., 2009, Middle to late Miocene chronostratigraphy and development of the northern Gulf of California: Marine Micropaleontology, v. 72, p. 10–25, doi:10.1016/j.marmicro.2009.02.003.

Herman, S.W., and Gans, P., 2006, A paleomagnetic investigation of large scale vertical axis rotations in coastal Sonora: evidence for transtensional proto-Gulf deformation: Geological Society of America Abstracts with Programs, v. 38, no. 7, p. 311.

Holt, J.W., Stock, J.M., and Holt, E.W., 2000, An age constraint on Gulf of California rifting from the Santa Rosalía basin, Baja California Sur, Mexico: Geological Society of America Bulletin, v. 112, p. 540–549, doi:10.1130/0016-7606(2000)112<540:AACOGO>2.0.CO;2.

House, P.K., Pearthree, P.A., and Perkins, M.E., 2008, Stratigraphic evidence for the role of lake spillover in the inception of the lower Colorado River in southern Nevada and western Arizona, *in* Reheis, M.C., et al., eds., Late Cenozoic drainage history of the southwestern Great Basin and lower Colorado River region: Geologic and biotic perspectives: Geological Society of America Special Paper 439, p. 335–353, doi:10.1130/2008.2439(15).

Jensky, W.A., 1975, Reconnaissance geology and geochronology of the Bahia de Banderas area, Nayarit and Jalisco, Mexico [M.S. thesis]: Santa Barbara, University of California–Santa Barbara, 80 p.

Karig, D.E., and Jensky, W., 1972, The proto-gulf of California: Earth and Planetary Science Letters, v. 17, p. 169–174, doi:10.1016/0012-821X(72)90272-5.

Keogh, M., 2010, Stratigraphic analysis of late Miocene to early Pliocene(?) sedimentary rocks, SW Isla Tiburón, Sonora, Mexico [B.S. thesis]: Eugene, University of Oregon, 76 p.

Lee, J., Miller, M., Crippen, R., Hacker, B., and Ledesma-Vazquez, J., 1996, Middle Miocene extension in the Gulf extensional province, Baja California: Evidence from the southern Sierra Juárez: Geological Society of America Bulletin, v. 108, p. 505–525, doi:10.1130/0016-7606(1996)108<0505:MMEITG>2.3.CO;2.

Lewis, C.J., and Stock, J.M., 1998, Paleomagnetic evidence of localized vertical-axis rotation during Neogene extension of the Sierra San Fermín, northeastern Baja California, Mexico: Journal of Geophysical Research, v. 103, p. 2455–2470, doi:10.1029/97JB02673.

Lomtatidze-Jiménez, E., 2013, Proveniencia y caracterizacion geoquemica e isotopica (Sm-Nd) de sedimentos en las cuencas del norte del Golfo de California [M.S. thesis]: Ensenada, B.C., Mexico, Centro de Investigación Científica y de Educación Superior de Ensenada, 118 p.

Lonsdale, P., 1989, Geology and tectonic history of the Gulf of California, *in* Winterer, E.L., et al., eds., The eastern Pacific Ocean and Hawaii: Boulder, Colorado, Geological Society of America, Geology of North America Volume N, p. 499–521.

Ludwig, K. R., 2003, Mathematical-statistical treatment of data and errors for Th-230/U geochronology: Uranium-Series Geochemistry, v. 52, p. 631–656.

Mar-Hernández, E., González-Escobar, M., and Martín-Barajas, A., 2012, Tectonic framework of Tiburon Basin, Gulf of California, from seismic reflection evidence: International Geology Review, v. 54, p. 1271–1283, doi:10.1080/00206814.2011.636988.

Martín-Barajas, A., Tellez-Duarte, M., and Stock, J.M., 1997, Pliocene volcaniclastic sedimentation along an accommodation zone in northeastern Baja California: The Puertecitos Formation, *in* Johnson, M.E., and Ledesma-Vasquez, J., eds., Pliocene carbonate and related facies flanking the Gulf of California, Baja California, Mexico: Geological Society of America Special Paper 318, p. 1–24, doi:10.1130/0-8137-2318-3.1.

Martín-Barajas, A., Vazquez-Hernandez, S., Carreno, A.L., Helenes, J., Suarez-Vidal, F., and Alvarez-Rosales, J., 2001, Late Neogene stratigraphy and tectonic control on facies evolution in the Laguna Salada Basin, northern Baja California, Mexico: Sedimentary Geology, v. 144, p. 5–35, doi:10.1016/S0037-0738(01)00133-6.

Martín-Barajas, A., González-Escobar, M., Fletcher, J.M., Pacheco, M., Oskin, M., and Dorsey, R., 2013, Thick deltaic sedimentation and detachment faulting delay the onset of continental rupture in the northern Gulf of California: Analysis of seismic reflection profiles: Tectonics, v. 32, p. 1294–1311, doi:10.1002/tect.20063.

McCloy, C., Ingle, J.C., and Barron, J.A., 1988, Neogene stratigraphy, foraminifera, diatoms, and depositional history of Maria Madre Island, Mexico: Evidence of early Neogene marine conditions in the southern Gulf of California: Marine Micropaleontology, v. 13, p. 193–212, doi:10.1016/0377-8398(88)90003-5.

McDougall, K., 2008, Late Neogene marine incursion and the ancestral Gulf of California, *in* Reheis, M., et al., eds., Late Cenozoic drainage history of the southwestern Great Basin and lower Colorado River region: Geologic and biotic perspectives: Geological Society of America Special Paper 439, p. 355–373, doi:10.1130/2008.2439(16).

McDougall, K., and Miranda Martínez, A.Y., 2014, Evidence for a marine incursion along the lower Colorado River corridor: Geosphere, v. 10, p. 842–869, doi:10.1130/GES00975.1.

McDougall, K., Poore, R.Z., and Matti, J.C., 1999, Age and environment of the Imperial Formation near San Gorgonio Pass, California: Journal of Foraminiferal Research, v. 29, p. 4–25.

Miller, N.C., and Lizarralde, D., 2013, Thick evaporites and early rifting in the Guaymas Basin, Gulf of California: Geology, v. 41, p. 283–286, doi:10.1130/G33747.1.

Miranda-Avilés, R., Beraldi-Campesi, H., Puy-Alquiza, M.J., and Carreño, A.L., 2005, Estromatolitos, tufas y travertinos de la sección El Morro: Depósitos relacionados con la primera incursión marina en la Cuenca de Santa Rosalía, Baja California Sur: Revista Mexicana de Ciencias Geológicas, v. 22, p. 148–158.

Molina-Cruz, A., 1994, Biostratigraphy and paleoceanographic significance of the radiolarians from the protomouth of the Gulf of California: Ciencias Marinas, v. 20, p. 441–465.

Nagy, E.A., and Stock, J.M., 2000, Structural controls on the continent-ocean transition in the northern Gulf of California: Journal of Geophysical Research, v. 105, p. 16,251–16,269, doi:10.1029/1999JB900402.

Nagy, E.A., Grove, M., and Stock, J.M., 1999, Age and stratigraphic relationships of pre- and syn-rift volcanic deposits in the northern Puertecitos Volcanic Province, Baja California, Mexico: Journal of Volcanology and Geothermal Research, v. 93, p. 1–30, doi:10.1016/S0377-0273(99)00080-3.

Neuhaus, J., 1989, Volcanic and nonmarine stratigraphy of southwest Isla Tiburón, Gulf of California, Mexico [M.S. thesis]: San Diego, California, San Diego State University, 170 p.

Niño-Estrada, L., Iriondo, A., García-Flores, R., McDowell, F.W., Izaguirre, A., Bennett, S.E.K., and Oskin, M.E., 2014, Edades Cretácicas de rocas batolíticas del Isla Tiburón, Golfo de California: Geochronología U-Pb en zircones mediante técnicas de ablación láser e ICP-MS: Proceedings Unión Geofísica Mexicana Reunión Anual, Puerto Vallarta, Mexico.

Ortlieb, L., 1991, Quaternary vertical movements along the coasts of Baja California and Sonora, *in* Dauphin, J.P., and Simoneit, B.R.T., eds., The Gulf and Peninsular Province of the Californias: American Association of Petroleum Geologists Memoir 47, p. 437–480, doi:10.1306/M47542C22.

Oskin, M., 2002, Tectonic evolution of the northern Gulf of California, Mexico, deduced from conjugate rifted margins of the upper Delfín Basin [Ph.D. thesis]: Pasadena, California Institute of Technology, 481 p.

Oskin, M., and Stock, J.M., 2003a, Marine incursion synchronous with plate-boundary localization in the Gulf of California: Geology, v. 31, p. 23–26, doi:10.1130/0091-7613(2003)031<0023:MISWPB>2.0.CO;2.

Oskin, M., and Stock, J.M., 2003b, Pacific–North America plate motion and opening of the Upper Delfín basin, northern Gulf of California: Geological Society of America Bulletin, v. 115, p. 1173–1190, doi:10.1130/B25154.1.

Oskin, M., Stock, J., and Martín-Barajas, A., 2001, Rapid localization of Pacific–North America plate motion in the Gulf of California: Geology, v. 29, p. 459–462, doi:10.1130/0091-7613(2001)029<0459:RLOPNA>2.0.CO;2.

Otvos, E.G., and Bock, W.D., 1976, Massive long-distance transport and redeposition of Upper Cretaceous planktonic foraminifers in Quaternary sediments: Journal of Sedimentary Petrology, v. 46, p. 978–984, doi:10.1306/212F70B3-2B24-11D7-8648000102C1865D.

Pacheco, M., Martín-Barajas, A., Elders, W., Espinosa-Cardena, J.M., Helenes, J., and Segura, A., 2006, Stratigraphy and structure of the Altar basin of NW Sonora: Implications for the history of the Colorado River delta and the Salton trough: Revista Mexicana de Ciencias Geológicas, v. 23, p. 22.

Petróleos Mexicanos (PEMEX), 1985, Proyecto de inversión San Felipe, estudio de evaluación de cuencas, prospecto San Felipe: México, Petróleos Mexicanos, Informe RNCH–008, 57 p.

Perch-Nielsen, K., 1985, Cenozoic calcareous nannofossils, *in* Bolli, H.M., et al., eds., Plankton stratigraphy: Volume 1, Planktic foraminifera, calcareous nannofossils and calpionellids: Cambridge University Press Earth Science Series, p. 427–554.

Postma, G., 1990, Depositional architecture and facies of river and fan deltas: A synthesis, *in* Colella, A., and Prior, D.B., eds., Coarse-grained deltas: International Association of Sedimentologists Special Publication 10, p. 13–27, doi:10.1002/9781444303858.ch2.

Ramos-Velázquez, E., Calmus, T., Valencia, V., Iriondo, A., Valencia-Moreno, M., and Bellon, H., 2008, U-Pb and $^{40}Ar/^{39}Ar$ geochronology of the coastal Sonora batholith: New insights on Laramide continental arc magmatism: Revista Mexicana de Ciencias Geológicas, v. 25, p. 314–333.

Schaaf, P., Roldan-Quintana, J., and Calmus, T., 1999, Terrane reconnaissance in NE Sonora, Mexico, in the light of Sr-Nd-Pb isotopic data from coastal belt granitoids: Eos (Transactions, American Geophysical Union), v. 80 (supplement), p. F1079–F1080.

Seiler, C., Fletcher, J.M., Quigley, M.C., Gleadow, A.J.W., and Kohn, B.P., 2010, Neogene structural evolution of the Sierra San Felipe, Baja California: Evidence for proto-Gulf transtension in the Gulf Extensional Province?: Tectonophysics, v. 488, p. 87–109, doi:10.1016/j.tecto.2009.09.026.

Simon, J.I., Renne, P.R., and Mundil, R., 2008, Implications of pre-eruptive magmatic histories of zircons for U-Pb geochronology of silicic extrusions: Earth and Planetary Science Letters, v. 266, p. 182–194, doi:10.1016/j.epsl.2007.11.014.

Slama, J., Kosler, J., Condon, D. J., Crowley, J.L., Gerdes, A., Hanchar, J.M., Horstwood, M.S.A., Morris, G.A., Nasdala, L., Norberg, N., Schaltegger, U., Schoene, B., Tubrett, M.N., and Whitehouse, M J., 2008, Plesovice zircon—A new natural reference material for U-Pb and Hf isotopic microanalysis: Chemical Geology, v. 249, no. 1-2, p. 1–35.

Smith, J.T., 1991, Cenozoic marine mollusks and paleogeography of the Gulf of California, *in* Dauphin, J.P., and Simoneit, B.R.T., eds., The Gulf and Peninsular Province of the Californias: American Association of Petroleum Geologists Memoir 47, p. 637–666, doi:10.1306/M47542C31.

Smith, J.T., Smith, J.G., Ingle, J.C.J., Gastil, R.G., Boehm, M.C., Roldan, Q.J., and Casey, R.E., 1985, Fossil and K-Ar age constraints on upper middle Miocene conglomerate, SW Isla Tiburón, Gulf of California: Geological Society of America Abstracts with Programs, v. 17, no. 6, p. 409.

Solari, L.A., Gómez-Tuena, A., Bernal, J.P., Pérez-Arvizu, O., and Tanner, M., 2010, U-Pb zircon geochronology with an integrated LA-ICP-MS microanalytical workstation: Achievements in precision and accuracy: Geostandards and Geoanalytical Research, v. 34, p. 5–18, doi:10.1111/j.1751-908X.2009.00027.x.

Stock, J.M., 1997, Age and source of pumice lapilli within the San Felipe marine sequence, northeast Baja California [abs.], *in* Proceedings, International Meeting on the Geology of the Baja California Peninsula, Ensenada, Baja California Norte, April 6–9, 1997: Ensenada, Baja California, Peninsular Geological Society, p. 98.

Stock, J.M., 2000, Relation of the Puertecitos Volcanic Province, Baja California, to development of the plate boundary in the Gulf of California, *in* Delgado-Granados, H., et al., eds., Cenozoic tectonics and volcanism of Mexico: Geological Society of America Special Paper 334, p. 143–155, doi:10.1130/0-8137-2334-5.143.

Stock, J.M., and Hodges, K.V., 1990, Miocene to recent structural development of an extensional accommodation zone, northeastern Baja California, Mexico: Journal of Structural Geology, v. 12, p. 315–328, doi:10.1016/0191-8141(90)90016-R.

Stock, J.M., Lewis, C.J., and Nagy, E.A., 1999, The Tuff of San Felipe: An extensive middle Miocene pyroclastic flow deposit in Baja California, Mexico: Journal of Volcanology and Geothermal Research, v. 93, p. 53–74, doi:10.1016/S0377-0273(99)00079-7.

Stock, J., Paz-Moreno, F.A., Martin, K., and Lin, D., 2006, The 12.5 Ma Tuff of San Felipe: A major structural marker horizon in northwestern Mexico [poster]: Ensenada, Mexico, Proceedings, Lithospheric Rupture in the Gulf of California–Salton Trough Region: National Science Foundation MARGINS RCL (Rupturing Continental Lithosphere) Workshop, 1 p., http://rcl-cortez.nsf-margins.org/Presentations/Cortez_Posters/Stock/STOCK.MARGINS.POSTERopt.pdf.

Stump, T.E., 1979, The evolutionary biogeography of the west Mexican Pectinidae (Mollusca: Bivalvia) [Ph.D. thesis]: San Diego, California, San Diego State University, 520 p.

Umhoefer, P.J., Dorsey, R.J., Willsey, S., Mayer, L., and Renne, P., 2001, Stratigraphy and geochronology of the Comondú Group near Loreto, Baja California Sur, Mexico: Sedimentary Geology, v. 144, p. 125–147, doi:10.1016/S0037-0738(01)00138-5.

Umhoefer, P.J., Schwennicke, T., Del Margo, M.T., Ruiz-Geraldo, G., Ingle, J.C., and McIntosh, W., 2007, Transtensional fault-termination basins: an important basin type illustrated by the Pliocene San Jose Island basin and related basins in the southern Gulf of California, Mexico: Basin Research, v. 19, p. 297–322, doi:10.1111/j.1365-2117.2007.00323.x.

Umhoefer, P., Skinner, L.A., Bennett, S.E.K., Oskin, M.E., Dorsey, R.J., and Darin, M.H., 2013, Breaching of transform faults and flooding of pull-apart basins to incrementally form the early Gulf of California seaway from ~8 to 6.3 Ma: Geological Society of America Abstracts with Programs, v. 45, no. 6, p. 15.

Van Eaton, A.R., Harper, M.A., and Wilson, C.J.N., 2013, High-flying diatoms: Widespread dispersal of microorganisms in an explosive volcanic eruption: Geology, v. 41, p. 1187–1190, doi:10.1130/G34829.1.

Winker, C.D., 1987, Neogene stratigraphy of the Fish Creek–Vallecito section, southern California: Implications for early history of the northern Gulf of California and Colorado Delta [Ph.D. thesis]: Tucson, University of Arizona, 494 p.

Withjack, M.O., and Jamison, W.R., 1986, Deformation produced by oblique rifting: Tectonophysics, v. 126, p. 99–124, doi:10.1016/0040-1951(86)90222-2.